THE GEOLOGICAL SOCIETY OF AMERICA®

BULLETIN

E: gsab@geosociety.org
W: geosociety.org/gsa
T: @geosociety

Kinematic and geodynamic evolution of the Panama Isthmus region: Implications for Central American Seaway closure

Tracking no: B35595R

Authors:
Rebecca McGirr (Australian National University), Maria Seton (University of Sydney), and Simon Williams (University of Sydney)

Abstract:
A major topic of debate in Earth and climate science surrounds the timing of closure of the Central American Seaway. While it is clear that the gateway was closed by ~2.8 Ma, recent studies based on geological and marine molecular evidence have suggested an earlier closing time of early to mid-Miocene. Here, we examine the influence of subduction and slab window formation on the time-varying paleoenvironments of the Panama Isthmus region. We develop detailed reconstructions of the seafloor-spreading history in the Panama Basin and incorporate previously published arc block rotations into a revised global plate model. Our reconstructions indicate that the Central American Seaway region has undergone multiple phases of slab window formation and migration, slab detachment and flat slab subduction since the Oligocene, while kinematically mapped slab windows agree well with slab gaps imaged in seismic tomography. In particular, we find that from the early Miocene, when there is clear evidence for Panama Isthmus emergence, the region was underlaid by a slab window. During the late Miocene, when there is evidence for intermittent arc deepening, and decreased transcontinental migration, we find an increase in subducted slab volumes beneath the Panama arc. Numerical and analogue models, and field observations, argue that slab windows can induce >1km of vertical uplift on the overriding plate. We therefore propose that this previously unexplored geodynamic mechanism can explain the variations in Panama Isthmus emergence, and intermittent shallow-water connections, reconciling alternative lines of evidence for Central American Seaway closure.

Kinematic and geodynamic evolution of the Panama Isthmus region: Implications for Central American Seaway closure

Rebecca McGirr[1,2], Maria Seton[1], and Simon Williams[1,3]

[1]EarthByte Group, School of Geosciences, University of Sydney, Sydney, NSW, Australia

[2]Research School of Earth Sciences, Australian National University, Canberra, ACT, Australia

[3]State Key Laboratory of Continental Dynamics, Department of Geology, Northwest University, Xi'an, China

ABSTRACT

A major topic of debate in Earth and climate science surrounds the timing of closure of the Central American Seaway. While it is clear that the gateway was closed by ~2.8 Ma, recent studies based on geological and marine molecular evidence have suggested an earlier closing time of early to mid-Miocene. Here, we examine the influence of subduction and slab window formation on the time-varying paleoenvironments of the Panama Isthmus region. We develop detailed reconstructions of the seafloor-spreading history in the Panama Basin and incorporate previously published arc block rotations into a revised global plate model. Our reconstructions indicate that the Central American Seaway region has undergone multiple phases of slab window formation and migration, slab detachment and flat slab subduction since the Oligocene, while kinematically mapped slab windows agree well with slab gaps imaged in seismic tomography. In particular, we find that from the early Miocene, when there is clear evidence for Panama Isthmus emergence, the region was underlaid by a slab window. During the late Miocene, when there is evidence for intermittent arc deepening, and decreased transcontinental migration, we find an

increase in subducted slab volumes beneath the Panama arc. Numerical and analogue models, and field observations, argue that slab windows can induce >1km of vertical uplift on the overriding plate. We therefore propose that this previously unexplored geodynamic mechanism can explain the variations in Panama Isthmus emergence, and intermittent shallow-water connections, reconciling alternative lines of evidence for Central American Seaway closure.

INTRODUCTION

The role of oceanic gateways in modulating Earth's climate has been extensively studied using both empirical and numerical approaches (e.g. Kennett, 1977; Sijp & England, 2004; von der Heydt & Dijkstra, 2008). The Central American Seaway or Panama Gateway is a type example of a gateway closure event but questions remain about the timing of closure (i.e. Montes et al., 2012; 2015; Bacon et al., 2013; 2015; O'Dea et al., 2016; Jaramillo et al., 2017). Various lines of evidence, primarily geological, paleontological, and molecular records, suggest different timing for initial seaway closure ranging from as early as 25 Ma (Bacon et al., 2013; 2015) to as recent as 2.8 Ma (O'Dea et al., 2016).

Evidence for an emergence of the Panama Isthmus and incipient gateway closure during the Pliocene has relied on sedimentary changes in isotopic, geochemical, and faunal signatures (e.g. Keigwin et al, 1978; Coates et al., 2004; O'Dea et al., 2016). Conclusions based on these constraints solely rely on the assumption that variations in proxy data are the result of gateway closure (Molnar, 2008). Recent geological and marine molecular evidence for an early to mid-Miocene gateway closure challenges the previously assumed first-order relationship between ocean circulation reorganisation and the timing of global climatic and biotic changes (Farris et al., 2011; Bacon et al., 2013; 2015; Montes et al., 2015; O'Dea et al., 2016).

Understanding the timing of gateway closure has important implications for the onset of thermohaline circulation, Northern Hemisphere Glaciation (NHG), the evolution of the Caribbean Sea, and the Great American Biotic Interchange (GABI) (Burton et al., 1997; Haug et al., 2001; Marshall et al., 1982; O'Dea et al., 2016). While the gateway was clearly closed by ~3 Ma, the question remains on whether the gateway endured periods of closure and opening prior to its unequivocal closure and if so, what are the drivers for these changes? Connections between plate kinematics, subduction characteristics and the geologic, geodynamic and seismic evolution of subduction zone systems within the Panama Isthmus region have been studied extensively, but the effect that these processes have on the timing of CAS closure and paleoceanographic effects remains unexplored.

In this paper, we use plate tectonic reconstructions and geophysical data to explore the subduction history of the Central American and Northern Andean margin, and thus whether geodynamic processes can resolve the conflicting timings for gateway closure that have previously been proposed. Specifically, we model the development and migration of slab window formation between 23 Ma to the present day by mapping the intersection of the spreading ridges from the Cocos and Nazca plates with the Middle American trench. Additionally, we explore end-member models of Central American arc block rotations and the timing of arc-continent collision. These processes have had a profound impact on the structure of the mantle, which we compare to images of mantle tomography, patterns of present-day seismicity and the evolution of arc magmatism and are coeval with timing of Panama gateway related events. Considering these two processes together may help reconcile some of the controversies on the timing of gateway closure.

The paper is organized as follows: first, we summarise existing knowledge of the present-day tectonic setting of the Panama region and the adjacent oceanic plates to the west. Next, we describe our revised reconstructions of the Early Cenozoic plate tectonic evolution of this region, combining onshore tectonic block motions from other studies with our own reinterpretation of the seafloor spreading history. We then use this reconstruction as the basis for quantifying the location and volume of oceanic lithosphere being subducted along the Panama Isthmus through time, and compare these estimates to seismic tomography models which image both the extent of past subduction zones and slab windows. Finally, we discuss the implications of our preferred reconstruction for the geodynamics of the Panama region, with a particular focus on how the time-dependent influence of slabs and slab windows beneath the Isthmus could have been an important, but rarely considered, controlling factor on the evolution of the Central American Seaway.

OVERVIEW OF THE PANAMA ISTHMUS AND SURROUNDING REGIONS

At present-day, the Panama Isthmus is surrounded by active and complex tectonics. The Cocos and Nazca plates subduct beneath the Caribbean and South American plates at the Middle American Trench (MAT) and Ecuador Trench (SAT) (Bird, 2003) (Fig. 1). Plate divergence is accommodated by the east trending Cocos-Nazca Spreading (CNS) system, and the north trending East Pacific Rise (EPR) (Bird, 2003) (Fig. 1). The Panama Fracture Zone (PFZ), an active transform fault, is the section of the CNS system currently being subducted, the point at which the PFZ intersects the trench represents the Panama triple junction (Johnston and Thorkelson, 1997; Bird, 2003) (Fig. 1). A recent study has hypothesised the existence of a microplate east of the PFZ, termed the Malpelo microplate (Fig. 1), separated from the Nazca plate to the south by a diffuse oceanic plate boundary, partially explaining previous failed

attempts to close the Cocos-Nazca-Pacific plate motion circuit (DeMets et al., 2010; Zhang et al., 2017).

Global reconstructions (e.g., Shephard et al., 2013; Müller et al., 2016) depict the western margin of the Americas as the site of continuous subduction since the Cretaceous. Oceanic crust preserved in the Pacific Basin suggests the existence of a large, continuous Farallon plate subducted beneath the Americas during the Eocene, but this plate broke into smaller plates (e.g. Cocos and Nazca) at 23 Ma (Hey, 1977; Barckhausen et al., 2001). Several studies have attempted to reconstruct the kinematics of Farallon plate fragmentation (Hey, 1977; Barckhausen et al., 2001), while few have attempted to reconstruct more recent, small scale fractionation of the Nazca plate in detail (Morell, 2015).

The Panama arc lies within the Panama microplate (i.e. Panama-Choco block; Fig. 1B) and initially formed as the result of Farallon plate subduction beneath the Caribbean plate from the Cretaceous during the westward motion of the North and South American plates (Buchs et al., 2010). Kinematic reconstructions of the region show initial arc-continent collision after 10 Ma (Pindell and Dewey, 1982), while Coates et al. (2004) suggested initial collision of the Panama arc at 12.8-9.5 Ma implied by a regional unconformity. The occurrence of east-west fracturing and changes in volcanic arc activity of the Panama arc from 25-23 Ma has recently been interpreted as evidence for initial arc-continent collision and the driving mechanism for constant and moderate uplift from the late Oligocene (Farris et al., 2011; Montes et al., 2012).

The eventual emergence of the Panama Isthmus resulted in the separation of the Pacific and Caribbean waters, closing the Central American Seaway (CAS) and connecting the North and South American landmasses. Abrupt changes in isotopic, geochemical and faunal assemblages preserved in sedimentary sequences on either side of the Isthmus have been used as

proxies for constraining the timing of gateway closure to between 7 and 2.8 Ma (Keigwin, 1978; Coates and Obando, 1996; Coates et al., 2004; O'Dea et al., 2016). Recent paleobiological data have been interpreted to support an older age for the emergence of a landbridge formed by 25-23 Ma (Bacon et al., 2013; 2015), while paleoceanographic studies suggested that the CAS was closed by 15-13 Ma (Sepulchre et al., 2014; Montes et al., 2015). These new interpretations have significant implications on our current understanding of the timing and causal relationships among environmental, ecological and evolutionary changes in the region.

Seafloor spreading in the central-eastern Pacific

While the northern and southern sections of the Cocos and Nazca plates, respectively, were created by east-west seafloor spreading at the EPR (Hey, 1977; Lonsdale, 2005; Morell, 2015) , the southern Cocos and northern Nazca crust preserve a more complex history involving Cocos-Nazca spreading. Magnetic anomaly patterns created by the CNS show a minimum of three major clockwise rotations in the orientation of the ridge-transform system (Barckhausen et al., 2001). The first rotation (CNS-1) refers to the oldest seafloor (~23-19.5 Ma), and only comprises a small region of crust containing northeast trending magnetic anomalies intersecting the trench on both the Cocos and Nazca plates (Barckhausen et al., 2001; Lonsdale, 2005). CNS-1 crust on the Cocos plate contains the 15 km wide Fisher Seamount Chain, and the 25 km wide Quepos Plateau within the Seamount Domain (SMD; Fig. 1), both of which lie >1 km above the adjacent seafloor (Morell, 2015).

The second rotation (CNS-2) spans ~19.5-14.5 Ma, and is located closer towards the CNS system (Barckhausen et al., 2001). CNS-2 crust contains several bathymetric features resultant from Cocos and Nazca plate movement over the Galapagos hotspot (Hey, 1977; Lonsdale and Klitgord, 1978). Located to the south of the SMD is a 200 km wide, 1000 km long track of the

Galapagos hotspot; the aseismic Cocos Ridge (Werner et al., 2003). The Cocos Ridge extends northeast from the CNS, north of the Galapagos Islands (GI), to the MAT, where it has been gradually subducted for the past 2-3 Myrs (Morell, 2015) (Fig. 1). The Cocos Ridge is truncated to the east by the PFZ, which is characterised by a ~2 km bathymetric scarp (Sandwell and Smith, 2009). To the south, the 600 km long, 300 km wide, aseismic Carnegie Ridge traces the eastward motion of the Nazca plate over the Galapagos hotspot. It extends to the SAT, however, it is yet to be subducted (Hey, 1977; Lonsdale and Klitgord, 1978; Lowrie et al., 1979).

Crust created from ~14.5 Ma to recent is representative of the third rotation (CNS-3), which has formed eastward trending magnetic anomalies, not yet intersecting the MAT (Atwater and Severinghaus, 1989; Barckhausen et al., 2001). Amongst this CNS-3 crust is the 25 km long extinct Morgan Rift (MoR), which is bound by 5-2 Ma magnetic anomalies, situated adjacent to the PFZ to the west (Lowrie et al., 1979) (Fig. 1).

The northeastern Nazca plate contains magnetic anomalies created by a network of extinct mid ocean ridges. These include the eastward trending, 400 km long Sandra Rift (SR), which is bound by ~8-13 Ma crust, increasing in age furthest from the ridge, and intersecting the SAT offshore Colombia (Lonsdale and Klitgord, 1978; Lonsdale, 2005) (Fig. 1). The 2 km high, 100 km wide, Coiba Ridge (CoR) is bound by the Balboa Fracture Zone (BFZ), and the Coiba Fracture Zone (CFZ), intersecting the margin offshore Panama to the east of the PFZ, characterised by ~2 km scarps, extending for more than 450 and 150 km, respectively (Lowrie et al., 1979) (Fig. 1). Unlike the BFZ, the CoR and CFZ are largely seismically inactive (Hey, 1977; Lonsdale and Klitgord, 1978; Lowrie et al., 1979). The origin of the CoR is largely speculative due to the absence of unambiguous magnetic anomalies, poor age constraints obtained from sediment samples, and a lack of rift structures that would suggest a Galapagos hot-

158 spot origin (Lonsdale, 2005; Morell, 2015). Alternative scenarios suggest geochemical signatures
159 of the CoR are related to the Galapagos hotspot, and that the CoR was originally attached to
160 either the Carnegie or Cocos Ridge before being rifted apart (Meschede and Barckhausen, 2001;
161 Hoernle et al., 2002; Werner et al., 2003). Lonsdale (2005) suggested that the CoR was produced
162 by tectonic tilting, and thus is not of hotspot origin.

163 Farther south, the northeastern Nazca plate contains the Malpelo Ridge (MaR), Malpelo
164 Rift (MR), Yaquina Graben (YG), and the Buenaventura Rift (BR) (Fig. 1). The MaR is ~420 km
165 wide, and has bathymetric and crustal thickness comparable to the Cocos Ridge (Hey, 1977;
166 Lonsdale and Klitgord, 1978; Sallarès et al., 2003). To the south, the extinct MR is bounded by
167 east to southeast trending ~15-9 Ma magnetic anomalies (Lonsdale and Klitgord, 1978).
168 Lonsdale and Klitgord (1978) propose that varied spreading rates between the MR and the
169 simultaneously spreading Costa Rica rift to the east resulted in an active transform boundary
170 south of the PFZ. Although not well understood, the extinct BR is postulated to exist east of the
171 MR, intersecting the SAT near Colombia (Hardy, 1991; Lonsdale, 2005). Assuming that the BR
172 existed, it was likely initially a segment of MR spreading, and is the result of a 12 Ma ridge
173 extinction caused by the attempted subduction of an oceanic scarp to the north, coeval with a
174 severe decrease in MR spreading rate (Lonsdale and Klitgord, 1978; Hardy, 1991; Lonsdale,
175 2005). The MR and YG are likely part of the same extinct spreading-transform system and could
176 be related to the SR to the north (Lonsdale, 2005).

177 **Alternative Cocos-Nazca slab geometries**

178 Several competing models exist for the evolution and present-day geometry of the Cocos
179 and Nazca subducted slabs beneath Central America and the Northern Andes (Fig. 2), primarily
180 based on present-day seismicity, volcanic arc characteristics (i.e. geochemistry and age), and

seismic wave velocities. These end-member scenarios of slab geometry have several implications for the evolution of large-scale geodynamic processes in the region. These include the absence of a subducting slab (i.e. a slab window) beneath Panama (Johnston and Thorkelson, 1997; Abratis and Wörner, 2001), flat-slab subduction under Columbia (Gutscher et al., 2000; Ramos and Folguera, 2009; Chiarabba et al., 2016; Idárraga-García et al., 2016; Wagner et al., 2017), and slab detachment beneath Central America (Rogers et al., 2002; Gazel et al., 2011).

The subducted Cocos slab is characterised by a steep dip (~80-60°) in the northwest portion, progressively shallowing to near horizontal along the Cocos Ridge axis (Protti et al., 1994). Abratis and Wörner (2001) suggested that the existence of young (<10 Ma) adakitic volcanism and patterns of seismicity within the southeastern portion of the slab indicate that a slab gap was formed at the leading edge of the Cocos Ridge soon after ridge-trench collision (Fig. 2B), either by slab break-off or subduction of a spreading centre. A later study argues that the Galapagos-like geochemical signature in magmas of southern Central America can only be explained by slab detachment of the Cocos plate, triggered by Cocos Ridge-MAT collision at ~10-8 Ma (Gazel et al., 2011) (Fig. 2A), or the attempted subduction of positively buoyant lithosphere at ~10-3.8 Ma (Rogers et al., 2002).

The geometry of the Nazca slab beneath Panama is poorly constrained, and many lines of evidence are not consistent with the presence of a subducting slab in the region (de Boer et al., 1991). Johnston and Thorkelson (1997) suggested that the subduction of a spreading ridge previously bound to the PFZ from ~8-2 Ma (Fig. 2B) produced a slab window between the Cocos and Nazca plates. Their hypothesis is based on the absence of a Wadati-Benioff zone from southern Costa Rica through to Central Panama, the occurrence of adakitic volcanism explained by anatectic melts of slab window edges, and the southward transition in volcanic arc

geochemistry from typical slab metasomatised, mid-ocean ridge basalt to ocean-island basalt derived from the upflow of Galapagos-enriched sub-slab mantle into the Panama arc source area. Other studies have suggested that initiation of left-lateral transform faulting south of Panama occurred in the late Oligocene to early Miocene (~38-23 Ma), supported by the gradual termination of arc magmatism (Lonsdale and Klitgord, 1978; Montes et al., 2012). This scenario would also result in the present-day absence of a subducting slab beneath eastern Panama.

Despite evidence of a slab window beneath Panama, many studies argue for an actively subducting slab in the region. This scenario is supported by the existence of a ~150 km offshore accretionary prism east of the PFZ, which is indicative of a history of oblique convergence (MacKay and Moore, 1990; Moore and Sender, 1995), while some have suggested that adakitic arc volcanism throughout Panama is evidence of a subducting Nazca slab (de Boer et al., 1988; Defant et al., 1992). In this case, the Nazca slab would likely be more steeply dipping than the adjacent Cocos slab, accommodated by a slab tear (Morell, 2015).

To the east, present-day Colombian earthquake depths and Holocene volcanism suggest the existence of a subducting flat slab (Gutscher et al., 2000) (Fig. 2C). The extent of the shallow-dipping slab suggests that it is being fed by eastward Nazca subduction to the south, south-eastward Caribbean subduction to the north, and underthrusting of the Panama arc due to active collision of the Panama-Choco block with South America (Idárraga-García et al., 2016). Farther south, the subducting Nazca slab dips more steeply (~60°), accommodated by the Caldas slab tear (Gutscher et al., 2000; Wagner et al., 2017). The extinct SR is hypothesised to be related to this Wadati-Benioff zone offset, suggesting that it formed along a zone of weakness (Chiarabba et al., 2016). Debate exists regarding the timing of slab shallowing, which likely initiated 13-9 Ma (Ramos and Folguera, 2009; Chiarabba et al., 2016; Wagner et al., 2017).

REVISED KINEMATIC RECONSTRUCTION OF THE CENTRAL AMERICAN SEAWAY REGION

We used the plate reconstruction software, GPlates (Müller et al., 2018) combined with magnetic anomaly data (Seton et al., 2014), bathymetric features such as fracture zone crossings (Matthews et al., 2011), aseismic ridges (Lonsdale, 2005) and fossil spreading centres (MacLeod et al., 2017) derived from satellite data (Sandwell and Smith, 2009) (Fig. 3 and 4) to visually reconstruct the Panama Isthmus region from the Oligocene (33.1 Ma) to recent.

Our reconstruction is implemented within a global hierarchy of plate motions, in contrast to previous studies that extrapolate present plate motions back in time (Johnston and Thorkelson, 1997; Morell, 2015; Meschede and Barckhausen, 2001). This means that our reconstruction accounts for changes in plate motion throughout the time period covered by our study, recorded by isochrons and fracture zones. Further, it allows us to reconstruct the plates with respect to structures in the underlying mantle using a mantle reference frame (Müller et al, 2016), suitable for linking the positions of tectonic features at the surface to structures in the mantle beneath.

Improvements to the block rotations of the Central American arc were made by adopting the rotations proposed in previous studies based on paleomagnetic analysis (Di Marco et al., 1995; Montes et al., 2012) (Fig. 5). We created a self-consistent network of continuously closing plate polygons (Gurnis et al., 2012) to define the dynamically evolving plate geometries both spatially and temporally. These refinements were incorporated into an early Mesozoic to present-day global plate reconstruction model (Müller et al., 2016).

The preferred magnetic anomaly identification compilation, fracture zones and associated global rotation model were used to produce improved seafloor-spreading isochrons for the eastern Pacific Ocean from 33.1 Ma. This process allows for a widespread interpretation and

representation of the age distribution of oceanic crust and its associated spreading regime through time. We used a global set of seafloor spreading isochrons defined by Müller et al. (2016) as the basis of our regional improvements. New seafloor-spreading isochrons were constructed for the CNS system at chrons 3n4o (5 Ma), 5o (10.9 Ma), 5Bo (15.16 Ma), 6o (20.10 Ma), 6Bo (23.07 Ma), consistent with the methodology of Müller et al. (2008). Additionally, 5Ao (12.4 Ma) isochrons were digitised for the Buenaventura, Malpelo and Sandra rift systems, and 8 Ma isochrons were created for the subducted ridge segments which were bound to the northernmost PFZ (Johnston and Thorkelson, 1997). As a significant proportion of CNS crust has been subducted, inferences on the age of subducted oceanic crust were made, based on the continental geological record to constrain the location of past plate boundaries, and the spreading regime deduced from presently preserved crust (Müller et al., 2016).

38-32 Ma

Oceanic crust along the East Pacific Rise (EPR) formed via spreading between the Pacific and Farallon plates, with crust that formed on the Pacific side currently residing in the south and southeast Pacific (Fig. 6) whereas parts of the crust that formed on the Farallon plate subducted beneath the Northern and Southern American plates (Fig. 6). Subduction of Farallon crust was continuous along the Americas from the late Cretaceous. During the late Eocene (~35 Ma), the EPR trended in a northwest direction, and seafloor spreading occurred in an ENE-SWS direction, consistent with the fracture zones in the area and the plate motions of Wright et al., (2016).

The Central American arc blocks were broadly linear during the late Eocene, trending in a NW-SE direction (Boschman et al., 2014). We implemented counterclockwise vertical-axis rotations of the Central Panama arc segments from 38-28 Ma, consistent with paleomagnetic

analyses of Central American volcanic arc rocks (Fig. 5) (Di Marco et al., 1995; Montes et al., 2012), which has implications for the location and geometry of subduction in the area.

32-23 Ma

From 32 Ma, seafloor spreading continued to be active along the EPR in an ENE-SWS direction, consistent with Farallon-Pacific plate motions of Wright et al. (2016). A ~275 km left-lateral strike slip fault developed offshore Central Panama between Middle and South America trench segments at 32 Ma, trending in an ENE direction, parallel to Farallon plate motion (Fig. 6). The development of a left-lateral strike-slip fault occurred within the hypothesised period of arc magmatism cessation in Central and Eastern Panama arc blocks (38-28 Ma) (Montes et al., 2012).

From 28 Ma, we implemented clockwise rotation of the central arc blocks, coeval with a brief renewal of arc magmatism in central Panama (Montes et al., 2012) (Fig. 5). Arc-continent collision occurred at 25 Ma initiating oroclinal tightening of the Central American arc (Montes et al., 2012). Collision replaced subduction between the Panama arc blocks and South America from 25 Ma, supported by late Oligocene deformation (Fig. 5 and 6) (Farris et al., 2011; Montes et al., 2012).

23-20 Ma

Break-up of the Farallon plate occured from ~23 Ma and the CNS system initiated in a northeast-southwest direction from ~23 Ma (CNS-1), causing the breakup of the Farallon plate into the smaller northeasterly moving Cocos plate to the north, and larger easterly moving Nazca plate to the south (Hey, 1977; Barckhausen et al., 2001) (Fig. 6). The fragmentation of the Farallon plate occurred via spreading along the Grijalva Scarp (Fig. 4), and lithospheric weakening due to passage over the Galapagos hotspot (Hey, 1977; Barckhausen et al., 2001).

The Grijalva Scarp defines the boundary between CNS-EPR crust on the Nazca plate, intersecting the South American Trench at present-day (Lonsdale and Klitgord, 1978; Barckhausen et al., 2001). This plate reconfiguration resulted in a ridge-ridge-ridge triple junction between the EPR and CNS system.

CNS-1 trended in a northeast direction (Barckhausen et al., 2001) and intersected the MAT south of central Panama, which caused a slab gap to form within the subducting Cocos plate (Fig. 6). Cocos-Nazca seafloor spreading occurred in a NNW-SSE direction from ~23-20 Ma, and the triple junction offshore central Panama moved northwest at a rate ~50 mm a^{-1}. Central American arc segments continued to tighten, accompanied by left-lateral strike-slip faulting offshore central Panama which resulted in an absence of Neogene volcanic arc magmatism (Montes et al., 2012).

20-15 Ma

A ridge jump from CNS-1 to CNS-2 at 20 Ma occurred via a clockwise rotation of the ridge-transform system (Barckhausen et al., 2001), which was accompanied by a change in seafloor spreading direction to NNE-SSW (Barckhausen et al., 2001; Lonsdale, 2005). The ridge-trench intersection was maintained between the CNS and MAT, which resulted in subduction of <3 Ma crust beneath central Panama, while the triple junction continued to travel northwest, however at a reduced rate of ~15 mm a^{-1}.

15-12 Ma

A third ridge jump from CNS-2 to CNS-3 occurred at 15 Ma via a clockwise rotation of the ridge-transform system, which trended in an east-west direction from thereon, and was accompanied by a north-south shift in spreading direction (Fig. 6) (Atwater and Severinghaus, 1989; Barckhausen et al., 2001). From 15 Ma, the east-stepping, northeast trending Malpelo and

Buenaventura spreading axes were initiated as a continuation of the CNS system to the east (Fig. 6). The direction of seafloor spreading of the Malpelo Rift (MR) and Buenaventura Rift (BR) occurred at an oblique angle to the east-west trending CNS segments. Variations in spreading rate between these two major systems lead to the development of an active transform boundary to the south (Lonsdale and Klitgord, 1978; Atwater and Severinghaus, 1989; Lonsdale, 2005).

A transform fault bound to the northern segments of the BR intersected the MAT offshore of southern Costa Rica, which travelled southeast at a rate of ~70 mm a^{-1}. We assumed that ridge-trench intersections did not occur from 15-8 Ma, and are instead replaced by transform-trench intersections, based on the assumption that fossil spreading centres near the SAT are an indication of plate fragmentation related to spreading centres stalling as they approached the trench (Johnston and Thorkelson, 1997).

12-9 Ma

From 12 Ma, the Sandra Rift (SR) was activated to the north of active Malpelo spreading segments as an east-west trending extension of the Cocos-Nazca axis, which propagated westward into older Cocos oceanic crust (Fig. 6). SR segments overlapped the BR segments, resulting in rift failure, and caused Malpelo spreading to slow from 12 Ma (Atwater and Severinghaus, 1989; Lonsdale, 2005). A right-lateral strike-slip fault joined CNS-3 segments with the SR to the north, forming a proto-PFZ. The intervening crust between the SR and MR spreading systems moved independently of Cocos and Nazca crust, forming the Malpelo microplate (Fig. 6). A second right-lateral transform boundary joined the MR and SR segments, forming the eastern boundary of the Malpelo Microplate. This transform boundary defines the first stage of Yaquina Graben (YG) development, which grew in length for the duration of the

Malpelo Microplate activity, and in width due to the formation of pull-apart basins (Hardy, 1991).

At ~12 Ma the aseismic Cocos and Malpelo Ridge axes were aligned, and the Malpelo Ridge was captured by the Malpelo Microplate, rifted from the Cocos Ridge to the east (Fig. 6). At 11 Ma, a small CNS ridge jump occurred (CNS-4) caused by a ~10° clockwise rotation (Atwater and Severinghaus, 1989). A fracture zone connected to the CNS intersected the MAT offshore southern Costa Rica and the triple junction continued to move southeast at a rate of ~70 mm a^{-1} from 12-10 Ma.

9-8 Ma

The CNS-4 rotated ~4° counterclockwise, and seafloor spreading continued in a NNE-SSW direction. The gradual slowing of the MR spreading caused its eventual cessation by ~9 Ma, the crust that formerly moved with the Malpelo Microplate was captured by the Nazca plate as a result (Fig. 6). Subsequently, right-lateral strike-slip motion along the eastern margin terminated, and the coalescence of pull-apart basins formed the modern YG (Hardy, 1991). SR spreading continued to the north (Lonsdale, 2005). The proto-PFZ grew due to spreading of the MR and SR concurrent to the adjacent Costa Rica rift segments, and subduction of the fracture zone intersecting the MAT continued. The Nazca segment of the Colombian flat slab started to shallow (Fig. 6), concurrent to Peruvian flat slab initiation farther south.

8-2 Ma

A fifth ridge jump (CNS-5) caused by a clockwise rotation (~4°) of the CNS occurred at ~8 Ma, which was accompanied by a north-south shift in seafloor spreading direction. To the east, a ridge jump occurred causing the cessation of the SR (Fig. 6), and the initiation of the east

stepping rift segments bound to the modern PFZ to the south, and intersecting the MAT offshore Costa Rica to the north (Johnston and Thorkelson, 1997). As a result, crust created by the SR was captured by the northern Nazca plate. Gradual subduction of the ridge-transform system beneath the Costa Rica-Panama border resulted in the formation of a slab gap mostly within the Nazca plate (Johnston and Thorkelson, 1997). By ~6 Ma the shallowing of the Columbian flat slab was complete.

2-0 Ma

From 2 Ma, Cocos-Nazca seafloor spreading continued in a north-south direction, and the CNS trended east-west. The PFZ was bound to the CNS to the east, and is currently being actively subducted by the MAT offshore southern Costa Rica (Johnston and Thorkelson, 1997). Crust currently subducted by the northern South America and southern Middle America Trenches is no younger than ~8 Ma.

SUBDUCTED SLAB VOLUMES AND SLAB WINDOWS

Reconstructions of the plate configurations and motions outlined above allow us to make quantitative estimates of past slab geometries along the Panama margin, incorporating estimates of the convergence rates and ages of the subducting seafloor. This subduction history is also recorded by present-day mantle structure imaged by seismological observations, providing an additional constraint with which to test the kinematic model. In this section we examine the Cenozoic history of subduction, and gaps in subduction, along the Panama margin and the level of agreement between kinematic reconstructions and seismological evidence.

The characteristics of subducting slab volumes are primarily influenced by trench geometries, plate velocities, convergence rates, slab dip, and the age of oceanic crust at the time of subduction. The formation of a gap in the subducting slab, referred to as a slab window, can

result from the intersection of diverging oceanic plates and trench segments during periods of uninterrupted subduction (Thorkelson, 1996). This process has been previously related to dynamic uplift, and anomalous magmatism and extension of the plate overriding a slab window (Breitsprecher and Thorkelson, 2009). The location and geometry of slab windows have previously been defined according to the ridge-transform-trench configuration, slab dip, and plate motion vectors (Thorkelson, 1996).

Global tomography modelling is a technique used for the visualisation of the Earth's interior via the interpretation of the observed seismic wavefield (van der Hilst et al., 1997). The seismic wavefield consists of a P-wave and two shear wave components. The velocities of these waves are determined by their first-order relationship with the temperature of the transmitting medium (van der Hilst et al., 1997). Thus, seismic velocity anomalies at depth are representative of regional variations in the seismic properties of the mantle. Global tomography models offer increasingly detailed constraints on mantle structure and convection due to continuously increasing data coverage and improved methodologies for seismic data processing and wave inversion (Li et al., 2008). However, the related uncertainty and resolution dependency of global tomography models, regardless of station coverage, is inhibited by the uneven sampling of mantle structures by seismic waves due to regions of seismic inactivity (van der Hilst et al., 1997; Li et al., 2008).

The spatial distribution of slab volumes within the mantle is dependent on the evolution of subduction zones and past surface plate velocities and configurations, thus, the analysis of seismic tomography models can be used to reconstruct the paleo-location of subduction zones with meaningful uncertainties (van der Meer et al., 2010). Slab detachment, slab windows, slab tears and past discontinuities in subduction can also be imaged by seismic tomography via the

identification of vertical and horizontal breaks in positive seismic velocity anomalies. These discontinuities have previously been correlated to epeirogenic uplift, regional variations in volcanic arc geochemistry and an absence of a well-defined Wadati-Benioff zone in the region, due to an influx of mantle asthenosphere between adjacent slab segments (Rogers et al., 2002; van Benthem et al., 2013).

In this section, we first kinematically reconstruct slab volumes beneath the Panama Isthmus region and Northern Andes by extracting the locations of trench segments and plate motion vectors from alternative plate models (Fig. S1-2) (Shephard et al., 2013; Müller et al., 2016), including our revised global plate reconstruction. We then identify the present-day location of remnant subducted slab material, slab gaps, and the presence of asthenospheric upwelling by determining what features are consistent between alternative models of seismic tomography most likely to reflect mantle temperature structure (Romanowicz, 2003) in the region.

Kinematic Reconstructions of slab distribution and slab windows

The evolution of plate motions, velocities and subduction in the Panama Isthmus region associated with the alternative kinematic models results in significantly different slab geometries and slab window locations, due to the location of ridge-trench intersections, or transform offsets, or a combination of these processes. The Shephard et al. (2013) reconstruction produces a slab window from 23 Ma, radiating from offshore Colombia where a ridge-trench intersection has been maintained since splitting off the Farallon plate (Fig. 7). The northeasterly motion and high velocity magnitude of Farallon and Cocos plate motions results in an even distribution of slab material beneath Central America, and a slightly higher volume of material beneath northwest South America due to slower Nazca plate velocities (Fig. 7). The age of subducted slab material

at the time of subduction ranges from 40-60 Myrs beneath Central America, increasing in age to the northwest (Fig. 7). Migration of the ridge-trench intersection northward offshore Panama by 15 Ma results in a similar migration of the slab window, residing under northwest South America, and the southern Caribbean by present-day (Fig. 7). The age of subducted slab material is youngest beneath Panama and Costa Rica (<10 Ma) due to the subduction of crust created by the CNS.

The Müller et al. (2016) reconstruction produces a much smaller slab window compared to the Shephard et al. (2013) model, as a result of CNS-intersection offshore Colombia from 23-16 Ma (Fig. 7). The volume of slab material beneath the northwest South American margin is significantly increased compared to Shephard et al. (2013), due to the addition of Caribbean subduction beneath South America. The migration of the ridge-trench intersection northward offshore southern Costa Rica results in slab window formation at 15-5 Ma, prior to the subduction of the PFZ. This slab window lies under southern Costa Rica through to east Panama within the Nazca plate, similar to the hypothesised slab window configuration of Johnston and Thorkelson (1997). The age of slab material at the time of subduction is youngest to the north of the slab window (Fig. 7).

Our revised reconstruction plots a slab window between northwest South America and Costa Rica due to ridge-trench intersection offshore Panama from 23-15 Ma (Fig. 7). The reduced extent of subduction along the northwest South American margin results in a significantly reduced volume of slab material compared to Müller et al. (2016). A transform-trench intersection replaces the ridge-trench intersection offshore at 15-8 Ma, creating an increased volume of slab material beneath central Panama at 8 Ma, although a slab window of reduced extent is maintained beneath east Panama as a result of left lateral strike-slip motion

(Fig. 7). In our kinematic model, a second ridge-trench intersection occurs between 8-2 Ma, resulting in the formation of a right-stepping slab window beneath southern Costa Rica, through to eastern Panama. The location of our slab window extends farther north than that predicted by Müller et al. (2016). Oblique subduction of the Nazca plate south of Central Panama is maintained from the initiation of transform offsets at 32 Ma, resulting in slab volumes beneath southern Panama, consistent with Johnston and Thorkelson (1997). Similar Cocos-Nazca plate motions to those in Shephard et al. (2013) result in a similar slab geometry and depth distribution beneath northern Central and South America. The oldest subducted crust in the region occurs beneath northern South America, consistent with Müller et al. (2016). Young subducted crust (<15 Ma) borders the slab window, currently being subducted beneath Panama and the Northern Andes.

Overall, our model shows a slab window that is larger, bounded by younger lithosphere, and farther north at ~15 Ma compared to previous models (Fig. 7). This is due to the offset introduced by implementing arc block rotations (Montes et al., 2012), and to some extent because the Müller et al. (2016) model had a lack of divergence between Cocos and Nazca after initial Farallon fragmentation. At present-day (Fig. 7), our model of slab window formation shows good agreement with the model of Johnston and Thorkelson (1997). Both our model and the Müller et al. (2016) model suggest the slab window is farther west than in the Shephard et al. (2013) model, while our model also suggests the age of subducting lithosphere is typically younger than in the other cases.

Vertical sections of seismic tomography

We analysed mantle images corresponding to several recent global P- and S-wave tomography models beneath Central America and northern South America, to identify which

anomalies were consistent between models (Table S1) in both horizontal and vertical slices. P-wave (compressional) velocity models are based on the two-way traveltime of seismic body waves, and are generally of higher lateral resolution, particularly in areas of dense seismic coverage, while S-wave (shear) models produce long-wavelength images of the mantle and are based on surface waves (Romanowicz, 2003). We present results for the MIT-P08 (Li et al., 2008) P-wave velocity model here (Fig. 8-9), while the results for the remaining models are presented in the supplementary material (Fig. S3-5). We interpreted positive (fast) seismic velocity anomalies to be representative of remnant subducted slab material, while negative (slow) velocity anomalies were interpreted as regions of upwelling in modelled mantle tomography. However, other processes (e.g. chemical or thermochemical) may alter imaged seismic wave perturbations (Romanowicz, 2003).

Profiles of seismic tomography were analysed to 1000 km depth, along three northeast striking profiles, perpendicular to the MAT along Central America, and one east striking profile, perpendicular to the SAT, intersecting the Colombian flat slab (Fig. 8). Vertical slices perpendicular to the strike of the trench were used for sampling seismic wave velocities along a profile to understand the history of subduction and characteristics of the downgoing slabs.

The MIT-P08 (Li et al., 2008) P-wave velocity model along Profile 1 images a prominent upper slab beneath the present-day location of the MAT, and lower flat slab material farther north (stagnating at the 660 km transition zone). These slab segments are separated by a slab gap between 250-500 km depth possibly resultant of slab detachment, as hypothesised by Rogers et al. (2002) (Fig. 8).

Farther south, Profile 2 transects Nicaragua and is characterised by a prominent, steeply dipping slab from 250 km depth in the MIT-P08 seismic tomography model. Rogers et al. (2002)

suggested that upper and lower slab segments occur in this region, similar to Profile 1 (Fig. 8). However this is not captured in the models analysed here, despite earthquake depth data suggesting the existence of an upper slab in this region (Rogers et al., 2002). Although Rogers et al. (2002) analysed P-wave tomography similar to the more recent MIT-P08 model, the reason for the discrepancy between these models is unclear but we note that the slab gap interpreted by Rogers et al. (2002) is also far less extensive in the other models we analysed (Fig. S3-5).

Profile 3 transects present-day strike slip motion offshore Panama, through central Panama and into the Caribbean where we expect to see a lack of subducting slab material based on the absence of a Wadati-Benioff zone from southeastern Costa Rica through Panama (Fig. 2). All analysed P-wave tomography models show an absence of dense mantle material in the upper mantle (Fig. 8 and S3-5). Instead, the majority of upper mantle material is composed of anomalously slow material, indicative of mantle upwelling.

The fourth profile extends over the SAT and the Colombian flat slab, in an east-west direction (Fig. 8). Upper slab material is not captured by any of the P-wave velocity models, however the depth of the slab in this region is very shallow (60 km) (Gutscher et al., 2000) and is unlikely to be captured. The subducting slab segment is located beneath the Northern Andes-South America boundary, where the leading edge of the Colombian flat slab is assumed to occur, based on earthquake hypocenter data (Gutscher et al., 2000). The subducting slab segments occur as an upper west dipping portion to 250 km depth, and lower steep-easterly dipping slab from 250 to 1000 km depth, below the Northern Andes (Fig. S3-5).

The mantle shear wave velocity model presented in the supplementary material (Fig. S5) (Grand, 2002) does not provide a good match to the finite frequency P-wave velocity anomaly models analysed in this section (Montelli et al., 2006; Li et al., 2008; Obayashi et al., 2013). The

distribution of dense mantle material is most consistent in the lower mantle, but poorly imaged in the upper mantle due to poor lateral resolutions of long wavelength S-wave models near subduction zones (Grand, 2002; Romanowicz, 2003).

Age-coded seismic tomography match to alternative kinematic models

The analysis of horizontal depth slices gives an indication of the location of paleo-subduction zones which we compare to alternative kinematic models, although not accounting for lower mantle thickening of slabs, unknown slab dip and tomographic imaging errors (van der Meer et al., 2010).

The northern segment of long-lived continuous Farallon subduction proposed by Müller et al. (2016), and implemented into our revised reconstruction, both based on Boschman et al. (2014) shows a good correlation with imaged slab material at ~881 km depth estimated to represent subduction at ~32 Ma. The occurrence of a subduction zone located between -75° and -78° longitude bound to a transform offset in our revised reconstruction produces the best fit to images of lower mantle structure. The scenario proposed by Shephard et al. (2013) based on Ross and Scotese (1988) also provides a good fit in this region at mid-mantle depths (Fig. 9), however, they are unable to account for the location of low velocity material beneath northern South America (Fig. 9).

Horizontal sections of seismic tomography image the opening of a gap in the Farallon slab by ~17 Ma (Fig. 9). The slab window is imaged between 8° and 12° latitude at 700 km depth (~17 Ma), growing in length parallel to trench segments. The location of ridge-trench intersections are maintained at the centre of slab window formation in our revised plate model. Both Shephard et al. (2013) and Müller et al. (2016) propose ridge-trench intersections too far south to explain slab gap formation in this region (Fig. 9). Within the upper mantle, slab volumes

along central and northern South America have decreased significantly, this is likely due to the effect of advective thickening in the lower mantle.

At mid-mantle depths (~8 Ma) slab volumes occur north of Costa Rica, inboard of Caribbean subduction and at the leading edge of Colombian flat slab subduction providing the best fit to our revised kinematic model (Fig. 9). Müller et al. (2016) depicts Nazca subduction beneath a southeastern segment of the Caribbean plate, unsupported by low velocity material, while Shephard et al. (2013) are unable to account for the existence of slab material beneath northwestern South America (Fig. 9).

DISCUSSION

Geodynamic evolution of the Panama Isthmus region

It has long been understood that the Panama Isthmus has been strongly affected by tectonic and geodynamic processes during its late Cenozoic history. However, the extent and spatio-temporal patterns of the influence of surface tectonics on the underlying mantle has been less well studied. Our analysis shows that the occurrence of discontinuous subduction in the Panama Isthmus region due to the initiation of left lateral strike-slip faulting from 32 Ma and generations of slab window formation beginning around 23 Myr ago, together with flat slab formation likely caused by the subduction of young, buoyant crust (Wagner et al., 2017), and the proximity of trench segments included in our revised kinematic model is able to explain a range of observations including present-day mantle structure inferred from seismic tomography.

Our revised kinematic model shows that the occurrence of a subduction zone located between -75° and -78° longitude bound to left lateral strike-slip motion to the north, and subduction between the Panamanian arc and northwest South America to the south from 32 Ma provides a good match to images of seismic tomography (Fig. 9). Farther north, along the Chortis

block and Costa Rica, our revised model provides the best match to the northwest striking, linear segment of anomalously fast perturbations, indicative of continuous Farallon subduction beneath the Americas prior to 32 Ma (Fig. 9).

The initiation of left lateral strike-slip faulting at ~32 Ma is consistent with the cessation of arc volcanism in eastern Panama, and produces a gap in subduction latitudinally consistent with images of seismic tomography (Fig. 9). Evidence for a temporary restart in arc volcanism throughout eastern Panama from 28-25 Ma has not been considered in our reconstruction (Montes et al., 2012), and evidence for a slab is similarly absent in imaged seismic tomography profiles sampled orthogonal to strike-slip faulting and slab gap formation (Fig. 8; Profile 3).

The kinematic reconstruction of Shephard et al (2013) fails to account for the occurrence of slab volumes beneath northwest South America as a result of southeast Caribbean subduction (Fig. 7 and 9). The Müller et al. (2016) kinematic model does capture the subduction of Caribbean crust below South America (Fig. 9), however, the occurrence of proximal trench segments to the east of the northwest South American margin to present-day is not represented in sections of seismic tomography (Fig. 9). Thus, we suggest that the cessation of this trench segment likely occurred after Panama-South America arc-continent collision at 25 Ma (Fig. 5). This timing is supported by the occurrence of east-west fracturing and a permanent change in Panama arc evolution (Farris et al., 2011; Montes et al., 2012). The location of the paleo-margin defined in our revised model is inconsistent with the zone of collision (Uramita suture), and realistically should strike north, defining the margin between the Northern Andes and Greater Panama.

In our revised model, a transform-trench triple junction is maintained offshore the Costa Rica-Panama border from 15-8 Ma, coeval with small scale fractionation of the Nazca plate (Fig.

593 6). Previous regional reconstructions that extrapolate present-day plate motions back in time
594 have assumed that the Sandra Rift intersects the SAT offshore Colombia during the mid-
595 Miocene (Morell, 2015). However, as an actively subducting flat slab exists in this area, made
596 evident by earthquake hypocenter data (Gutscher et al., 2000) (Fig. 2), we instead propose that
597 Malpelo Rift and Sandra Rift segments are connected to the MAT via a proto-PFZ which is
598 propagated within young, weak oceanic crust (Fig. 6). The configuration of this ridge-trench
599 reorganisation is consistent with the available magnetic anomalies in the area (Fig. 3) and images
600 of seismic tomography (Fig. 8-9), however, either interpretation is to some extent conjectural
601 based on extrapolation of preserved seafloor.

602 Images of seismic tomography show discontinuous Cocos slab subduction in our northern
603 profiles. The northernmost profile depicts a slab gap between 410-250 km depth, and farther
604 south, the Cocos slab does not extend to the surface, present at depths greater than 250 km (Fig.
605 8). The imaged gap in slab volumes has previously been related to slab detachment and incipient
606 uplift of the Central American plateau between ~10 and 3.8 Ma, possibly due to the attempted
607 subduction of buoyant lithosphere (Rogers et al., 2002), while others suggested that slab
608 detachment is the result of Cocos Ridge-MAT collision during the Upper Miocene (~10-8 Ma)
609 (Abratis and Wörner, 2001; Gazel et al., 2011), however more recent tectonic reconstructions
610 suggested that Cocos Ridge collision did not occur until ~3-2 Ma (Morell, 2015). As each of the
611 alternative kinematic models depict continuous Cocos subduction beneath Central America to
612 present-day, the distribution of Cocos slab material in the upper mantle is inconsistent with
613 images of seismic tomography (Fig. 7-9).

614 The geometry of the late Miocene to recent slab window within the subducting Cocos
615 slab implemented into our kinematic model differs from some previous hypotheses for slab

window or slab gap formation in the region (Fig. 6 and 7). Abratis and Wörner (2001) hypothesise slab window formation at the leading edge of Cocos Ridge subduction due to the subduction of a ridge-transform system from ~8 Ma. They suggested that slab window formation is coeval with cessation of mantle-wedge derived arc volcanism, later replaced by alkalic and adakitic backarc lavas with geochemical signatures derived from the Galapagos plume (de Boer et al., 1995). This signature has been interpreted by Gazel et al. (2011) to be the result of slab detachment at the leading edge of the aseismic Cocos Ridge due to the removal of the slab-pull force causing flattening of the upper slab segment.

Our interpretation for the absence of subducting segments in the Panama Isthmus region is consistent with those of Johnston and Thorkelson (1997), who suggest that a slab window formed due to the subduction of a ridge-transform system bound to the northern PFZ from ~8-2 Ma, consistent with the absence of a Wadati-Benioff zone beneath the region, the occurrence of adakitic volcanism (mantle-wedge source metasomatized by slab derived melts), and alkalic volcanism (Galapagos plume signature). Conversely, the southern slab window edge implemented in our kinematic model lies farther north compared to Johnston and Thorkelson (1997), as their model would require northward-younging magnetic anomalies on the northern Nazca plate offshore (Abratis and Wörner, 2001). Additionally, persistent oblique subduction of the Nazca plate east of the PFZ maintained to present-day explains the existence of a ~150 km offshore accretionary prism, previously interpreted as evidence for active oblique Nazca subduction beneath Panama (MacKay and Moore, 1990; Moore and Sender, 1995).

The position of slab gaps in the mid and upper mantle are predicted well by our kinematic model when left lateral strike-slip motion south of Panama is initiated at 32 Ma, accompanied by persistent ridge-trench intersections offshore of the Costa Rica-Panama border from 23-15 Ma,

and 8-2 Ma (Fig. 7 and 9). Both Shephard et al. (2013) and Müller et al. (2016) model ridge-trench intersections much farther south of the gradual opening of a slab gap centred at 9° latitude imaged in horizontal sections of mantle tomography during the first iteration of slab window opening (Fig. 7 and 9). As both the Shephard et al. (2013) and Müller et al. (2016) kinematic models fail to capture an absence of subducting slab material above 660 km depth below central Panama (Fig. 7), we consider these to be the least representative models (of those analysed as part of this study) for the region from the late Eocene to recent.

The kinematic reconstructions of slab volumes using our revised reconstruction to better explain the structure of the mantle as imaged by seismic tomography than previous reconstructions that follow a global plate hierarchy (Shephard et al., 2013; Müller et al., 2016), due to our consideration of the location of ridge-trench intersections and the initiation of strike-slip motion from ~32 Ma (Montes et al, 2012). Our revised reconstruction fits the available observations from mantle tomography to the same degree as previous detailed reconstructions of the Panama Isthmus region focussed on the late Miocene to present (i.e. Morell, 2015; Johnston and Thorkelson, 1997). But in addition, we suggest that multiple generations of slab window formation together with the initiation of strike-slip motion resulting in discontinuous subduction beneath Panama from the late Eocene, and Colombian flat slab subduction, are necessary to explain the geodynamic evolution of subducted slab volumes beneath Panama and northwest South America imaged by seismic tomography (Fig. 8 and 9).

Implications of slab windows beneath Panama for Mantle-induced vertical motions

The development of slabs and slab windows beneath the Panama region has implications for unravelling the history of surface motions. Previous studies based on both field observations, and analogue and numerical modelling, have shown that mantle upwelling associated with slab

windows can lead to significant, transient dynamic (non-isostatic) topography on the overriding plate. Studies from Patagonia (Fosdick et al., 2013; Guillaume et al., 2013), the West Antarctic Peninsula (Guenthner et al., 2010), and Alaska (Benowitz et al., 2012) have used low-temperature thermochronology to interpret 1-3 km of rapid uplift associated with ridge-trench intersections and slab window migration. Analogue studies of vertical motions above slab windows have suggested that a transient topographic signature of 1-5 km of uplift is expected on the overriding plate, due to the absence of sinking slab material, and the channeling of asthenospheric mantle through the slab window (Guillaume et al., 2010). Additionally, these studies suggested that the asthenospheric mantle channeled through the slab window does not mix with supra-slab material (Guillaume et al., 2010), and explains the occurrence of anomalous oceanic island basalt-type volcanism above slab windows. This is observed throughout Panama and southern Costa Rica above the hypothesised location of a slab window from ~8-2 Ma (de Boer et al., 1991; 1995; Johnston and Thorkelson, 1997), and other regions globally, where active spreading regions presently intersect zones of subduction (e.g. Patagonian Andes; Breitsprecher and Thorkelson, 2009; Guillaume et al., 2009; Ramos, 2005). Thermo-mechanical numerical models of ridge subduction and slab window formation (i.e. Groome and Thorkelson, 2009) have supported the findings of field and analogue studies, adding that ridge-trench intersections and incipient slab window formation manifests as rapid exhumation in the forearc region of the overriding plate.

Our reconstructions of the subduction history along the western margin of the Panama region imply that dynamic uplift due to migrating slab windows could have played a significant role in modulating surface topography, beginning with the splitting of the Farallon plate into the Nazca and Cocos plates ~23 Myr ago and continuing to present day. If we assume that the slab

window-induced uplift in Panama were of a similar order of magnitude as in other regions, we could expect km-scale changes in dynamic topography for Central Panama, coeval with the occurrence of slab windows as implemented into our kinematic model. Our results support an up-down-up signature in vertical motion through the Neogene, correlating with two generations of persistent ridge-trench intersections offshore Central Panama separated by an intervening period with reduced upwelling as deeper slab material lies close to the transform-trench intersection (Fig. 7, 8 Ma). Indeed, a recent thermochronology study of the Panama Isthmus region (Ramírez et al., 2016) suggests that the final emergence of the Isthmus was the result of two regionally extensive uplift events during the middle and late Miocene. The two phases of uplift would be consistent with sedimentary evidence for two distinct periods of arc emergence, interrupted by significant intermittent arc deepening (O'Dea et al., 2016). We propose that the kinematic model of the region could also be improved by implementing flat slab subduction beneath the Cordillera de Talamanca, inboard of the aseismic Cocos Ridge (Gardner et al., 2013; Morell, 2015), and by replicating slab tear formation at the leading edge of Cocos Ridge subduction from ~8 Ma (Gazel et al., 2011). Further insights could also be drawn from more detailed seismic imaging of the mantle beneath Panama - while existing tomography models show good agreement with the existence of slab windows since ~23 Ma (Fig. 8 and 9), these models are unable to resolve small-scale details predicted by our kinematic model.

Implications for Central American Seaway closure

Debate continues to surround the topic of Central American Seaway (CAS) closure due to various lines of conflicting evidence, primarily geological, paleontological, and molecular records. Interpretations of initial seaway closure timing range from early Oligocene to mid-Miocene (Bacon et al., 2013; 2015; Montes et al., 2015; Jaramillo et al., 2017) to as recent as 2.8

708 Ma (i.e. O'Dea et al., 2016). An understanding of the historical vertical motions of the Panama
709 arc as a result of the kinematic and geodynamic evolution of the region is necessary in clarifying
710 the timing of CAS closure.

711 Arc-continent-collision along Panama occurred at ~25 Ma, driving tectonic shortening
712 and emergence of the northern Andes and Panama arc blocks, consistent with east-west
713 fracturing of Panama arc blocks, and a shift in volcanic arc activity (Farris et al., 2011; Montes et
714 al., 2012). After initial arc-continent collision, moderate uplift is recorded in sedimentary
715 sequences throughout Panama, generally highest near the Uramita suture in the Darien Province
716 (Montes et al., 2012). This recorded uplift is coeval with the widening of a slab gap that we
717 modelled in this study (Fig. 10), and subduction of young, relatively buoyant seafloor beneath
718 Panama due to the interaction between the Cocos-Nazca Spreading Centre and the MAT in our
719 revised reconstruction, which could have contributed to local uplift, or reduced the impact of
720 regional dynamic subsidence caused by the continuously subducting Cocos plate farther north.

721 Montes et al. (2015) suggested that fluvial Eocene zircons of a uniquely "Panamanian"
722 signature arrived at the Magdalena Basin in northwest South America by the middle Miocene
723 (Fig. 10), implying that a Caribbean-Pacific connection between South America and Greater
724 Panama had ended by ~15-13 Ma. This coincides with a well-developed slab window with
725 related upwelling potentially supporting the emergence of the Panama Isthmus by the middle
726 Miocene (Fig. 10). Arc uplift is further evident in a shift from deepwater biogenic sedimentation
727 to a sequence of shallowing and coarsening upward siliciclastics and turbiditic sequences by 15
728 Ma within the Darien Province (Coates et al., 2004). A shallow and transient seawater
729 connection was present west of the Canal basin (Montes et al., 2015), on the northern flank of
730 slab window opening prior to 15 Ma in our revised reconstruction.

Bacon et al. (2013; 2015) propose an early Miocene formation of a land bridge, shortly after arc-continent collision explaining dispersal events that predate the majority of migrations associated with the GABI, consistent with Oligocene arc-continent collision (Farris et al., 2011), and fluvial connections between Panama and northwest South America by the middle Miocene (Montes et al., 2015). By ~12 Ma, a statistically significant shift in the rate of phylogenetic lineage-dispersals occurs, indicative of a decrease in transcontinental flora and fauna migrations (Jaramillo et al., 2017). This event has been related to no known geological or environmental driver (O'Dea et al., 2016), however, it does occur prior to a recorded interruption in arc uplift at 10 Ma (Fig. 10). The interruption is then succeeded by 3 Myrs of temporary, but significant, arc deepening recorded by a change in the age and depth of sedimentary units across the Panama arc, unexplained by eustatic sea-level estimates (Miller et al., 2005; O'Dea et al., 2016). This event coincides with active spreading along Malpelo and Sandra rift segments, and transform-trench intersections offshore Central Panama which would have resulted in the reintroduction of slab volumes beneath parts of Central Panama (Fig. 7 and 10).

Our kinematic reconstructions indicate that a period of arc deepening, unexplained by isostatic or sea-level drivers, could result from transient changes in mantle support beneath Panama, with dynamic uplift associated with the early Miocene slab window disrupted by increasing dynamic subsidence associated with slab material located beneath Central Panama from 15-9 Ma (Fig. 7) (however, strike-slip motion to the south causes a continued absence of slab material beneath eastern Panama). Previous studies have implied that land rafting could be the cause of earlier migrations (Pinto-Sánchez et al., 2012; O'Dea et al., 2016), however this assumption does not provide a mechanism for a sudden decrease in terrestrial migrations

753 (Jaramillo et al., 2017). We propose instead that the mechanism was geodynamic, a consequence
754 of the time-dependence of subduction and migration of ridge-trench intersections.
755 Panama arc uplift is gradually resumed from 6 Ma, ~2 Myrs after the proposed
756 subduction of a right-stepping ridge-transform system bound to the CNS, beneath Central
757 Panama (Fig. 10) (Johnston and Thorkelson, 1997). A second shift in the rate of dispersal-
758 vicariance indicates an increase in migration at ~3 Ma coincident with drastic eustatic sea-level
759 fall, caused by increased NADW production, and incipient increases in evaporation and
760 precipitation, driving the expansion of Arctic ice sheets from 3.15 Ma (Fig. 10) (Bartoli et al.,
761 2005; Bacon et al., 2013; O'Dea et al., 2016). These events coincide with the divergence of
762 Caribbean and tropical eastern Pacific planktonic assemblages and carbonate accumulation rates,
763 an increased contrast in surface ocean salinity, and steepening of the eastern Pacific thermohaline
764 temperature gradient during the Pliocene (Fig. 10) (O'Dea et al., 2016). This is consistent with
765 the hypothesis that Caribbean and Pacific shallow water connections existed, although
766 intermittently, through passages other than the CAS (i.e north of the Canal basin) from 15 to
767 ~3.5 Ma (Montes et al., 2015).
768 Considering the substantial evidence for a complex history of Cocos-Nazca subduction
769 presented in this study, the emergence of the Panama Isthmus would have been sensitive to small
770 fluctuations in dynamic uplift or subsidence, even at lower amplitudes for over 10 Myrs. A
771 geodynamic mechanism for variations in Panama Isthmus emergence, and intermittent shallow-
772 water connections provides an explanation for variations in dispersal rates and the
773 inconclusiveness of paleoceanographic proxy data.

CONCLUSIONS

This study examines the connection between plate kinematics, subduction characteristics and the geologic, geodynamic and seismic evolution of subduction zone systems within the Panama Isthmus region within the context of Central American Seaway closure. Our revised kinematic model includes multiple generations of Central American arc block rotations and oroclinical tightening, ridge-trench intersections offshore Costa Rica and Panama, flat slab subduction beneath Colombia from 9 Ma and captures periods of seafloor spreading along fossil rift systems within the northern Panama Basin.

A reconstruction with strike-slip motion south of Panama from 32 Ma combined with ridge-trench intersections from 23-15 Ma, and 8-2 Ma, implemented into our reconstruction resulted in the formation of a more extensive slab window extending from southern Costa Rica through to eastern Panama than in alternative reconstructions, and provides the most consistent explanation for gaps in subducted material imaged by seismic tomography above 660 km depth beneath Panama. When considering that the formation of a slab window can induce between 1-5 km of uplift, we conclude that variations in Panama Isthmus emergence, and intermittent shallow-water connections can be explained by a previously unexplored geodynamic mechanism. This mechanism provides an explanation for variations in dispersal rates and the inconclusivity of paleoceanographic proxy data, and may help resolve some of the controversies surrounding the timing of Central American Seaway closure.

ACKNOWLEDGMENTS

RM was funded by an AGRTP and Dean’s Merit scholarships while MS was funded through Australian Research Council Grant FT130101564. SW acknowledges support from ARC grants IH130200012 and DP180102280.

REFERENCES CITED

Abratis, M., and Wörner, G., 2001, Ridge collision, slab-window formation, and the flux of Pacific asthenosphere into the Caribbean realm: Geology, v. 29, no. 2, p. 127–130, https://doi.org/10.1130/0091-7613(2001)029<0127:RCSWFA>2.0.CO;2.

Atwater, T., and Severinghaus, J., 1989, Tectonic maps of the northeast Pacific, *in* Winterer, E.L., Hussong, D.M., and Decker, R.W., eds., The eastern Pacific Ocean and Hawaii, Geological Society of America, Geology of North America, v. N, p. 15–20, https://doi.org/10.1130/DNAG-GNA-N.15.

Bacon, C.D., Mora, A., Wagner, W.L., and Jaramillo, C.A., 2013, Testing geological models of evolution of the Isthmus of Panama in a phylogenetic framework: Botanical Journal of the Linnean Society, v. 171, no. 1, p. 287–300, https://doi.org/10.1111/j.1095-8339.2012.01281.x.

Bacon, C.D., Silvestro, D., Jaramillo, C., Smith, B.T., Chakrabarty, P., and Antonelli, A., 2015, Biological evidence supports an early and complex emergence of the Isthmus of Panama: Proceedings of the National Academy of Sciences, v. 112, no. 19, p. 6110–6115, https://doi.org/10.1073/pnas.1423853112.

Barckhausen, U., Ranero, C.R., von Huene, R., Cande, S.C., and Roeser, H.A., 2001, Revised tectonic boundaries in the Cocos Plate off Costa Rica: Implications for the segmentation of the convergent margin and for plate tectonic models: Journal of Geophysical Research: Solid Earth, v. 106, no. B9, p. 19207–19220, https://doi.org/10.1029/2001JB000238.

Bartoli, G., Sarnthein, M., Weinelt, M., Erlenkeuser, H., Garbe-Schönberg, D., and Lea, D.W., 2005, Final closure of Panama and the onset of northern hemisphere glaciation: Earth and Planetary Science Letters, v. 237, no. 1–2, p. 33–44,

https://doi.org/10.1016/j.epsl.2005.06.020.

Benowitz, J.A., Haeussler, P.J., Layer, P.W., O'Sullivan, P.B., Wallace, W.K., and Gillis, R.J., 2012, Cenozoic tectono-thermal history of the Tordrillo Mountains, Alaska: Paleocene-Eocene ridge subduction, decreasing relief, and late Neogene faulting: Geochemistry, Geophysics, Geosystems, v. 13, no. 4, https://doi.org/10.1029/2011GC003951.

Bird, P., 2003, An updated digital model of plate boundaries: Geochemistry, Geophysics, Geosystems, v. 4, no. 3, https://doi.org/10.1029/2001GC000252.

Boschman, L.M., van Hinsbergen, D.J., Torsvik, T.H., Spakman, W., and Pindell, J.L., 2014, Kinematic reconstruction of the Caribbean region since the Early Jurassic: Earth-Science Reviews, v. 138, p. 102–136, https://doi.org/10.1016/j.earscirev.2014.08.007.

Breitsprecher, K., and Thorkelson, D.J., 2009, Neogene kinematic history of Nazca–Antarctic–Phoenix slab windows beneath Patagonia and the Antarctic Peninsula: Tectonophysics, v. 464, no. 1–4, p. 10–20, https://doi.org/10.1016/j.tecto.2008.02.013.

Buchs, D.M., Arculus, R.J., Baumgartner, P.O., Baumgartner-Mora, C., and Ulianov, A., 2010, Late Cretaceous arc development on the SW margin of the Caribbean Plate: Insights from the Golfito, Costa Rica, and Azuero, Panama, complexes: Geochemistry, Geophysics, Geosystems, v. 11, no. 7, https://doi.org/10.1029/2009GC002901.

Burton, K.W., Ling, H.F., and O'Nions, R.K., 1997, Closure of the Central American Isthmus and its effect on deep-water formation in the North Atlantic: Nature, v. 386, no. 6623, p. 382–385, https://doi.org/10.1038/386382a0.

Chiarabba, C., De Gori, P., Faccenna, C., Speranza, F., Seccia, D., Dionicio, V., and Prieto, G.A., 2016, Subduction system and flat slab beneath the Eastern Cordillera of Colombia: Geochemistry, Geophysics, Geosystems, v. 17, no. 1, p. 16–27,

https://doi.org/10.1002/2015GC006048.

Coates, A.G., and Obando, J.A., 1996, The geologic evolution of the Central American Isthmus, *in* Jackson, J.B.C., Budd, A.F., and Coates, A.G., eds., Evolution and environment in tropical America, University of Chicago Press, Chicago, Illinois, p. 21–56.

Coates, A.G., Collins, L.S., Aubry, M.P., and Berggren, W.A., 2004, The geology of the Darien, Panama, and the late Miocene-Pliocene collision of the Panama arc with northwestern South America: Geological Society of America Bulletin, v. 116, no. 11–12, p. 1327–1344, https://doi.org/10.1130/B25275.1.

de Boer, J.Z., Defant, M.J., Stewart, R.H., Restrepo, J.F., Clark, L.F, and Ramirez, A.H., 1988, Quaternary calc-alkaline volcanism in western Panama: regional variation and implication for the plate tectonic framework: Journal of South American Earth Sciences, v. 1, no. 3, p. 275–293, https://doi.org/10.1016/0895-9811(88)90006-5.

de Boer, J.Z., Defant, M.J., Stewart, R.H., and Bellon, H., 1991, Evidence for active subduction below western Panama: Geology, v. 19, no. 6, p. 649–652, https://doi.org/10.1130/0091-7613(1991)019<0649:EFASBW>2.3.CO;2.

de Boer, J.Z., Drummond, M.S., Bordelon, M.J., Defant, M.J., Bellon, H., and Maury, R.C., 1995, Cenozoic magmatic phases of the Costa Rican island arc (Cordillera de Talamanca), *in* Mann, P., ed., Geologic and tectonic development of the Caribbean plate boundary in southern Central America, Geological Society of America Special Paper 295, Boulder, Colorado, p. 35–55.

Defant, M.J., Jackson, T.E., Drummond, M.S., de Boer, J.Z., Bellon, H., Feigenson, M.D., Maury, R.C., and Stewart, R.H., 1992, The geochemistry of young volcanism throughout western Panama and southeastern Costa Rica: an overview: Journal of the Geological

Society, v. 149, no. 4, p. 569–579, https://doi.org/10.1144/gsjgs.149.4.0569.

DeMets, C., Gordon, R.G., and Argus, D.F., 2010, Geologically current plate motions: Geophysical Journal International, v. 181, no. 1, p. 1–80, https://doi.org/10.1111/j.1365-246X.2009.04491.x.

Di Marco, G., Baumgartner, P.O., and Channell, J.E.T., 1995, Late Cretaceous-early Tertiary paleomagnetic data and a revised tectonostratigraphic subdivision of Costa Rica and western Panama, *in* Mann, P., ed., Geologic and tectonic development of the Caribbean plate boundary in southern Central America, Geological Society of America Special Paper 295, Boulder, Colorado, p. 1–27.

Eakins, B.W., and Lonsdale, P.F., 2003, Structural patterns and tectonic history of the Bauer microplate, Eastern Tropical Pacific: Marine Geophysical Researches, v. 24, no, 3–4, p. 171–205, https://doi.org/10.1007/s11001-004-5882-4.

Farris, D.W., Jaramillo, C., Bayona, G., Restrepo-Moreno, S.A., Montes, C., Cardona, A., Mora, A., Speakman, R.J., Glascock, M.D., and Valencia, V., 2011, Fracturing of the Panamanian Isthmus during initial collision with South America: Geology, v. 39, no. 11, p. 1007–1010, https://doi.org/10.1130/G32237.1.

Ferrari, L., Orozco-Esquivel, T., Manea, V., and Manea, M., 2012, The dynamic history of the Trans-Mexican Volcanic Belt and the Mexico subduction zone: Tectonophysics, v. 522, p. 122–149, https://doi.org/10.1016/j.tecto.2011.09.018.

Fosdick, J.C., Grove, M., Hourigan, J.K., and Calderon, M., 2013, Retroarc deformation and exhumation near the end of the Andes, southern Patagonia: Earth and Planetary Science Letters, v. 361, p. 504–517, https://doi.org/10.1016/j.epsl.2012.12.007.

Gardner, T.W., Fisher, D.M., Morell, K.D., and Cupper, M.L., 2013, Upper-plate deformation in

response to flat slab subduction inboard of the aseismic Cocos Ridge, Osa Peninsula, Costa Rica: Lithosphere, v. 5, no. 3, p. 247–264, https://doi.org/10.1130/L251.1.

Gazel, E., Hoernle, K., Carr, M.J., Herzberg, C., Saginor, I., van den Bogaard, P., Hauff, F., Feigenson, M., and Swisher III, C., 2011, Plume–subduction interaction in southern Central America: Mantle upwelling and slab melting: Lithos, v. 121, no. 1–4, p. 117–134, https://doi.org/10.1016/j.lithos.2010.10.008.

Grand S.P., 2002, Mantle shear-wave tomography and the fate of subducted slabs: Philosophical Transactions of the Royal Society of London, v. A360, no. 1800, p. 2475–2491, https://doi.org/10.1098/rsta.2002.1077.

Groome, W.G., and Thorkelson, D.J., 2009, The three-dimensional thermo-mechanical signature of ridge subduction and slab window migration: Tectonophysics, v. 464, no. 1–4, p. 70–83, https://doi.org/10.1016/j.tecto.2008.07.003.

Guenthner, W.R., Barbeau Jr, D.L., Reiners, P.W., and Thomson, S.N., 2010, Slab window migration and terrane accretion preserved by low-temperature thermochronology of a magmatic arc, northern Antarctic Peninsula: Geochemistry, Geophysics, Geosystems, v. 11, no. 3, https://doi.org/10.1029/2009GC002765.

Guillaume, B., Martinod, J., Husson, L., Roddaz, M., and Riquelme, R., 2009, Neogene uplift of central eastern Patagonia: Dynamic response to active spreading ridge subduction?: Tectonics, v. 28, no. 2, https://doi.org/10.1029/2008TC002324.

Guillaume, B., Moroni, M., Funiciello, F., Martinod, J., and Faccenna, C., 2010, Mantle flow and dynamic topography associated with slab window opening: Insights from laboratory models: Tectonophysics, v. 496, no. 1–4, p. 83–98, https://doi.org/10.1016/j.tecto.2010.10.014.

912 Guillaume, B., Gautheron, C., Simon-Labric, T., Martinod, J., Roddaz, M., and Douville, E.,
913 2013, Dynamic topography control on Patagonian relief evolution as inferred from low
914 temperature thermochronology: *Earth and Planetary Science Letters*, v. *364*, p. 157–167,
915 https://doi.org/10.1016/j.epsl.2012.12.036.
916 Gurnis, M., Turner, M., Zahirovic, S., DiCaprio, L., Spasojevic, S., Müller, R.D., Boyden, J.,
917 Seton, M., Manea, V.C., and Bower, D.J., 2012, Plate tectonic reconstructions with
918 continuously closing plates: Computers & Geosciences, v. 38, no. 1, p. 35–42,
919 https://doi.org/10.1016/j.cageo.2011.04.014.
920 Gutscher, M.A., Spakman, W., Bijwaard, H., and Engdahl, E.R., 2000, Geodynamics of flat
921 subduction: Seismicity and tomographic constraints from the Andean margin: Tectonics,
922 v. 19, no. 5, p. 814–833, https://doi.org/10.1029/1999TC001152.
923 Handschumacher, D.W., 1976, Post-Eocene plate tectonics of the eastern Pacific: The
924 Geophysics of the Pacific Ocean Basin and its margin, v. 19, p. 177–202,
925 https://doi.org/10.1029/GM019p0177.
926 Hardy, N.C., 1991, Tectonic evolution of the easternmost Panama Basin: Some new data and
927 inferences: Journal of South American earth sciences, v. 4, no. 3, p. 261–269,
928 https://doi.org/10.1016/0895-9811(91)90035-J.
929 Haug, G.H., Tiedemann, R., Zahn, R., and Ravelo, A.C., 2001, Role of Panama uplift on oceanic
930 freshwater balance: Geology, v. 29, no. 3, p. 207–210, https://doi.org/10.1130/0091-
931 7613(2001)029<0207:ROPUOO>2.0.CO;2.
932 Hey, R., 1977, Tectonic evolution of the Cocos-Nazca spreading center: Geological Society of
933 America Bulletin, v. 88, no. 12, p. i–vi, https://doi.org/10.1130/0016-
934 7606(1977)882.0.CO;2.

Hoernle, K., van den Bogaard, P., Werner, R., Lissinna, B., Hauff, F., Alvarado, G., and Garbe-Schönberg, D., 2002, Missing history (16–71 Ma) of the Galápagos hotspot: Implications for the tectonic and biological evolution of the Americas: Geology, v. 30, no. 9, p. 795–798, https://doi.org/10.1130/0091-7613(2002)030<0795:MHMOTG>2.0.CO;2.

Idárraga-García, J., Kendall, J.M., and Vargas, C.A., 2016, Shear wave anisotropy in northwestern South America and its link to the Caribbean and Nazca subduction geodynamics: Geochemistry, Geophysics, Geosystems, v. 17, no. 9, p. 3655–3673, https://doi.org/10.1002/2016GC006323.

Jaramillo, C., Montes, C., Cardona, A., Silvestro, D., Antonelli, A., and Bacon, C.D., 2017, Comment (1) on "Formation of the Isthmus of Panama" by O'Dea et al.: Science Advances, v. 3, no. 6, p. e1602321, https://doi.org/10.1126/sciadv.1602321.

Johnston, S.T., and Thorkelson, D.J., 1997, Cocos-Nazca slab window beneath central America: Earth and Planetary Science Letters, v. 146, no. 3–4, p. 465–474, https://doi.org/10.1016/S0012-821X(96)00242-7.

Kameo, K., and Sato, T., 2000, Biogeography of Neogene calcareous nannofossils in the Caribbean and the eastern equatorial Pacific—floral response to the emergence of the Isthmus of Panama: Marine Micropaleontology, v. 39, no. 1–4, p. 201–218, https://doi.org/10.1016/S0377-8398(00)00021-9.

Keigwin Jr, L.D., 1978, Pliocene closing of the Isthmus of Panama, based on biostratigraphic evidence from nearby Pacific Ocean and Caribbean Sea cores: Geology, v. 6, no. 10, p. 630–634, https://doi.org/10.1130/0091-7613(1978)6<630:PCOTIO>2.0.CO;2.

Keigwin, L., 1982, Isotopic paleoceanography of the Caribbean and East Pacific: role of Panama uplift in late Neogene time: Science, v. 217, no. 4557, p. 3503–353,

https://doi.org/10.1126/science.217.4557.350.

Kellogg, J.N., and Vega, V., 1995, Tectonic development of Panama, Costa Rica, and the Colombian Andes: constraints from global positioning system geodetic studies and gravity, *in* Mann, P., ed., Geologic and tectonic development of the Caribbean plate boundary in southern Central America, Geological Society of America Special Paper 295, Boulder, Colorado, p. 75–90.

Kennett, J.P., 1977, Cenozoic evolution of Antarctic glaciation, the circum-Antarctic Ocean, and their impact on global paleoceanography: Journal of geophysical research, v. 82, no. 27, p. 3843–3860, https://doi.org/10.1029/JC082i027p03843.

Klitgord, K.D., and Mammerickx, J., 1982, Northern East Pacific Rise: magnetic anomaly and bathymetric framework: Journal of Geophysical Research: Solid Earth, v. 87, no. B8, p. 6725–6750, https://doi.org/10.1029/JB087iB08p06725.

Lear, C.H., Rosenthal, Y., and Wright, J.D., 2003, The closing of a seaway: ocean water masses and global climate change: Earth and Planetary Science Letters, v. 210, no. 3–4, p. 425–436, https://doi.org/10.1016/S0012-821X(03)00164-X.

Li, C., van der Hilst, R.D., Engdahl, E.R., and Burdick, S., 2008, A new global model for P wave speed variations in Earth's mantle: Geochemistry, Geophysics, Geosystems, v. 9, no. 5, https://doi.org/10.1029/2007GC001806.

Lonsdale, P., and Klitgord, K.D., 1978, Structure and tectonic history of the eastern Panama Basin: Geological Society of America Bulletin, v. 89, no. 7, p. 981–999, https://doi.org/10.1130/0016-7606(1978)89<981:SATHOT>2.0.CO;2.

Lonsdale, P., 2005, Creation of the Cocos and Nazca plates by fission of the Farallon plate: Tectonophysics, v. 404, no. 3–4, p. 237–264, https://doi.org/10.1016/j.tecto.2005.05.011.

Lowrie, A., Aitken, T., Grim, P., and McRaney, L., 1979, Fossil spreading center and faults within the Panama fracture zone: Marine Geophysical Researches, v. 4, no. 2, p. 153–166, https://doi.org/10.1007/BF00286402.

MacKay, M.E., and Moore, G.F., 1990, Variation in deformation of the south Panama accretionary prism: Response to oblique subduction and trench sediment variation: Tectonics, v. 9, no. 4, p. 683–698, https://doi.org/10.1029/TC009i004p00683.

MacLeod, S.J., Williams, S.E., Matthews, K.J., Müller, R.D., and Qin, X., 2017, A global review and digital database of large-scale extinct spreading centers: Geosphere, v. 13, no. 3, p. 911–949, https://doi.org/10.1130/GES01379.1.

Marshall, L.G., Webb, S.D., Sepkoski, J.J., and Raup, D.M., 1982, Mammalian evolution and the great American interchange: Science, v. 215, no. 4538, p. 1351–1357, https://doi.org/10.1126/science.215.4538.1351.

Matthews, K.J., Müller, R.D., Wessel, P., and Whittaker, J.M., 2011, The tectonic fabric of the ocean basins: Journal of Geophysical Research: Solid Earth, v. 116, no. B12, https://doi.org/10.1029/2011JB008413.

Meschede, M., and Barckhausen, U., 2001, The relationship of the Cocos and Carnegie ridges: age constraints from paleogeographic reconstructions: International Journal of Earth Sciences, v. 90, no. 2, p. 386–392, https://doi.org/10.1007/s005310000155.

Miller, K.G., Kominz, M.A., Browning, J.V., Wright, J.D., Mountain, G.S., Katz, M.E., Sugarman, P.J., Cramer, B.S., Christie-Blick, N. and Pekar, S.F., 2005, The Phanerozoic record of global sea-level change: *Science*, v. *310*, no. 5752, p. 1293–1298, https://doi.org/10.1126/science.1116412.

Molnar, P., 2008, Closing of the Central American Seaway and the Ice Age: A critical review:

Paleoceanography, v. 23, no. 2, https://doi.org/10.1029/2007PA001574.

Montelli, R., Nolet, G., Dahlen, F.A., and Masters, G., 2006, A catalogue of deep mantle plumes: New results from finite-frequency tomography: Geochemistry, Geophysics, Geosystems, v. 7, no. 11, https://doi.org/10.1029/2006GC001248.

Montes, C., Bayona, G., Cardona, A., Buchs, D.M., Silva, C.A., Morón, S., Hoyos, N., Ramírez, D.A., Jaramillo, C.A., and Valencia, V., 2012, Arc-continent collision and orocline formation: Closing of the Central American seaway: Journal of Geophysical Research: Solid Earth, v. 117, no. B4, https://doi.org/10.1029/2011JB008959.

Montes, C., et al., 2015, Middle Miocene closure of the Central American seaway: Science, v. 348, no. 6231, p. 226–229, https://doi.org/10.1126/science.aaa2815.

Moore, G.F., and Sender, K.L., 1995, Fracture zone collision along the South Panama margin, *in* Mann, P., ed., Geologic and tectonic development of the Caribbean plate boundary in southern Central America, Geological Society of America Special Paper 295, Boulder, Colorado, p. 201–213.

Morell, K.D., 2015, Late Miocene to recent plate tectonic history of the southern Central America convergent margin: Geochemistry, Geophysics, Geosystems, v. 16, no. 10, p. 3362–3382, https://doi.org/10.1002/2015GC005971.

Müller, R.D., Sdrolias, M., Gaina, C., and Roest, W.R., 2008, Age, spreading rates, and spreading asymmetry of the world's ocean crust: Geochemistry, Geophysics, Geosystems, v. 9, no. 4, https://doi.org/10.1029/2007GC001743.

Müller, R.D., et al., 2016, Ocean basin evolution and global-scale plate reorganization events since Pangea breakup: Annual Review of Earth and Planetary Sciences, v. 44, p. 107–138, https://doi.org/10.1146/annurev-earth-060115-012211.

Müller, R.D., Cannon, J., Qin, X., Watson, R.J., Gurnis, M., Williams, S., Pfaffelmoser, T., Seton, M., Russell, S.H., and Zahirovic, S., 2018, GPlates: Building a virtual Earth through deep time: Geochemistry, Geophysics, Geosystems, v. 19, no. 7, p. 2243–2261, https://doi.org/10.1029/2018GC007584.

Newkirk, D.R., and Martin, E.E., 2009, Circulation through the Central American Seaway during the Miocene carbonate crash: Geology, v. 37, no. 1, p. 87–90, https://doi.org/10.1130/G25193A.1.

O'Dea, A., Lessios, H.A., Coates, A.G., Eytan, R.I., Restrepo-Moreno, S.A., Cione, A.L., Collins, L.S., De Queiroz, A., Farris, D.W., Norris, R.D., and Stallard, R.F., 2016, Formation of the Isthmus of Panama: Science advances, v. 2, no. 8, p. e1600883, https://doi.org/10.1073/pnas.1423853112.

Obayashi, M., Yoshimitsu, J., Nolet, G., Fukao, Y., Shiobara, H., Sugioka, H., Miyamachi, H., and Gao, Y., 2013, Finite frequency whole mantle P wave tomography: Improvement of subducted slab images: Geophysical Research Letters, v. 40, no. 21, p. 5652–5657, https://doi.org/10.1002/2013GL057401.

Pindell, J., and Dewey, J.F., 1982, Permo-Triassic reconstruction of western Pangea and the evolution of the Gulf of Mexico/Caribbean region: Tectonics, v. 1, no. 2, p. 179–211, https://doi.org/10.1029/TC001i002p00179.

Pinto-Sánchez, N.R., Ibáñez, R., Madriñán, S., Sanjur, O.I., Bermingham, E., and Crawford, A.J., 2012, The great American biotic interchange in frogs: multiple and early colonization of Central America by the South American genus Pristimantis (Anura: Craugastoridae): Molecular Phylogenetics and Evolution, v. 62, no. 3, p. 954–972, https://doi.org/10.1016/j.ympev.2011.11.022.

Protti, M., Gu, F., and McNally, K., 1994, The geometry of the Wadati-Benioff zone under southern Central America and its tectonic significance: Results from a high-resolution local seismographic network: Physics of the Earth and Planetary Interiors, v. 84, no. 1–4, p. 271–287, https://doi.org/10.1016/0031-9201(94)90046-9.

Ramírez, D.A., Foster, D.A., Min, K., Montes, C., Cardona, A. and Sadove, G., 2016, Exhumation of the Panama basement complex and basins: Implications for the closure of the Central American seaway: Geochemistry, Geophysics, Geosystems, v. 17, no. 5, p. 1758–1777, https://doi-org.virtual.anu.edu.au/10.1002/2016GC006289.

Ramos, V.A., 2005, Seismic ridge subduction and topography: Foreland deformation in the Patagonian Andes: Tectonophysics, v. 399, no. 1–4, p. 73–86, https://doi.org/10.1016/j.tecto.2004.12.016.

Ramos, V.A., and Folguera, A., 2009, Andean flat-slab subduction through time: Geological Society, London, Special Publications, v. 327, no. 1, p. 31–54, https://doi.org/10.1144/SP327.3.

Righter, K., 1997, High bedrock incision rates in the Atenguillo river valley, Jalisco, western Mexico: Earth Surface Processes and Landforms: The Journal of the British Geomorphological Group, v. 22, no. 4, p. 337–343, https://doi.org/10.1002/(SICI)1096-9837(199704)22:4<337::AID-ESP684>3.0.CO;2-1.

Righter, K., Caffee, M., Rosas-Elguera, J., and Valencia, V., 2010, Channel incision in the Rio Atenguillo, Jalisco, Mexico, defined by 36Cl measurements of bedrock: Geomorphology, v. 120, no. 3–4, p. 279–292, https://doi.org/10.1016/j.geomorph.2010.04.001.

Rogers, R.D., Kárason, H., and van der Hilst, R.D., 2002, Epeirogenic uplift above a detached slab in northern Central America: Geology, v. 30, no. 11, p. 1031–1034,

https://doi.org/10.1130/0091-7613(2002)030<1031:EUAADS>2.0.CO;2.

Romanowicz, B., 2003, Global mantle tomography: progress status in the past 10 years: Annual Review of Earth and Planetary Sciences, v. 31, no. 1, p. 303–328, https://doi.org/10.1146/annurev.earth.31.091602.113555.

Ross, M.I., and Scotese, C.R., 1988, A hierarchical tectonic model of the Gulf of Mexico and Caribbean region: Tectonophysics, v. 155, no. 1–4, p. 139–168, https://doi.org/10.1016/0040-1951(88)90263-6.

Sallarès, V., Charvis, P., Flueh, E.R., and Bialas, J., 2003, Seismic structure of Cocos and Malpelo Volcanic Ridges and implications for hot spot-ridge interaction: Journal of Geophysical Research: Solid Earth, v. 108, no. B12, https://doi.org/10.1029/2003JB002431.

Sandwell, D.T., and Smith, W.H., 2009, Global marine gravity from retracked Geosat and ERS-1 altimetry: Ridge segmentation versus spreading rate: Journal of Geophysical Research: Solid Earth, v. 114, no. B1, https://doi.org/10.1029/2008JB006008.

Sepulchre, P., Arsouze, T., Donnadieu, Y., Dutay, J.C., Jaramillo, C., Le Bras, J., Martin, E., Montes, C., and Waite, A.J., 2014, Consequences of shoaling of the Central American Seaway determined from modeling Nd isotopes: Paleoceanography, v. 29, no. 3, p. 176–189, https://doi.org/10.1002/2013PA002501.

Seton, M., Whittaker, J.M., Wessel, P., Müller, R.D., DeMets, C., Merkouriev, S., Cande, S., Gaina, C., Eagles, G., Granot, R., and Stock, J., 2014, Community infrastructure and repository for marine magnetic identifications: Geochemistry, Geophysics, Geosystems, v. 15, no. 4, p. 1629–1641, https://doi.org/10.1002/2013GC005176.

Shephard, G.E., Müller, R.D. and Seton, M., 2013, The tectonic evolution of the Arctic since

Pangea breakup: Integrating constraints from surface geology and geophysics with mantle structure: Earth-Science Reviews, v. 124, p. 148–183, https://doi.org/10.1016/j.earscirev.2013.05.012.

Sijp, W.P., and England, M.H., 2004, Effect of the Drake Passage throughflow on global climate: Journal of Physical Oceanography, v. 34, no. 5, p. 1254–1266, https://doi.org/10.1175/1520-0485(2004)034<1254:EOTDPT>2.0.CO;2.

Stephenson, S.N., Roberts, G.G., Hoggard, M.J., and Whittaker, A.C., 2014, A Cenozoic uplift history of Mexico and its surroundings from longitudinal river profiles: Geochemistry, Geophysics, Geosystems, v. 15, no. 12, p. 4734–4758, https://doi.org/10.1002/2014GC005425.

Thorkelson, D.J., 1996, Subduction of diverging plates and the principles of slab window formation: Tectonophysics, v. 255, no. 1–2, p. 47–63, https://doi.org/10.1016/0040-1951(95)00106-9.

Torsvik, T.H., Müller, R.D., Van der Voo, R., Steinberger, B., and Gaina, C., 2008, Global plate motion frames: toward a unified model: Reviews of geophysics, v. 46, no. 3, https://doi.org/10.1029/2007RG000227.

van Benthem, S., Govers, R., Spakman, W., and Wortel, R., 2013, Tectonic evolution and mantle structure of the Caribbean: Journal of Geophysical Research: Solid Earth, v. 118, no. 6, p. 3019–3036, https://doi.org/10.1002/jgrb.50235.

van der Hilst, R.D., Widiyantoro, S., and Engdahl, E.R., 1997, Evidence for deep mantle circulation from global tomography: Nature, v. 386, no. 6625, p. 578–584, https://doi.org/10.1038/386578a0.

van der Meer, D.G., Spakman, W., van Hinsbergen, D.J., Amaru, M.L. and Torsvik, T.H., 2010,

Towards absolute plate motions constrained by lower-mantle slab remnants: Nature Geoscience, v. 3, no. 1, p.36–40, https://doi.org/10.1038/ngeo708.

von der Heydt, A. and Dijkstra, H.A., 2008, The effect of gateways on ocean circulation patterns in the Cenozoic: Global and Planetary Change, v. 62, no. 1–2, p. 132–146, https://doi.org/10.1016/j.gloplacha.2007.11.006.

Wagner, L.S., Jaramillo, J.S., Ramírez-Hoyos, L.F., Monsalve, G., Cardona, A., and Becker, T.W., 2017, Transient slab flattening beneath Colombia: Geophysical Research Letters, v. 44, no. 13, p. 6616–6623, https://doi.org/10.1002/2017GL073981.

Werner, R., Hoernle, K., Barckhausen, U., and Hauff, F., 2003, Geodynamic evolution of the Galápagos hot spot system (Central East Pacific) over the past 20 my: Constraints from morphology, geochemistry, and magnetic anomalies: Geochemistry, Geophysics, Geosystems, v. 4, no. 12, https://doi.org/10.1029/2003GC000576.

Wright, N.M., Seton, M., Williams, S.E., and Mueller, R.D., 2016, The Late Cretaceous to recent tectonic history of the Pacific Ocean basin: Earth-Science Reviews, v. 154, p. 138–173, https://doi.org/10.1016/j.earscirev.2015.11.015.

Zhang, T., Gordon, R.G., Mishra, J.K., and Wang, C., 2017, The Malpelo plate hypothesis and implications for nonclosure of the Cocos-Nazca-Pacific plate motion circuit: Geophysical Research Letters, v. 44, no. 16, p. 8213–8218, https://doi.org/10.1002/2017GL073704.

FIGURE CAPTIONS

Figure 1. (A) Bathymetry and topography of Central America and northern South America and (B) regional gravity map (Sandwell and Smith, 2014). Present-day plate boundaries, modified from Bird (2003) (black), coastlines (grey), fracture zones (white) (Matthews et al., 2011), extinct ridges (blue) (Macleod et al., 2017), possible fossil spreading (blue, dashed) (Hardy,

1991). Rough Smooth Boundary (RSB; dashed); Cordillera de Talamanca (CT); Canal Basin (CB); Darien Ranges (DR); Magdalena Basin (MB); Llanos Basin (LB); Eastern Cordillera (EC); Central Cordillera (CC); Western Cordillera (WC); Malpelo Ridge (MaR); Cocos Ridge (CoR); Seamount Domain (SMD); Middle America Trench (MAT); North Panama Deformed Belt (NPDB); Panama Fracture Zone (PFZ); Morgan Rift (MoR); Balboa Fracture Zone (BFZ); Coiba Fracture Zone (CFZ); Sandra Rift (SR); possible Malpelo Microplate (MM?); Buenaventura Rift (BR); Yaquina Graben (YG); Malpelo Rift (MR); South America Trench (SAT); Cocos-Nazca Spreading centre (CNS).

Figure 2. (Top) Location of present-day earthquakes and active subduction related arc volcanism (red triangles) and adakitic volcanism (black triangles). (A) Cocos slab gap (Rogers et al., 2002), (B) alternative models of present-day slab window geometry, Abratis and Wörner 2001 (1); Johnston and Thorkelson 1997 (2), (C) Colombian flat slab (Gutscher et al., 2000). Abbreviations and line colours the same as Fig. 1 except Panama (PM); Northern Andes (NA).

Figure 3. Preferred set of magnetic anomaly picks for the Panama Basin (Cocos and Nazca plates). Abbreviations and lines the same as Fig. 1 except fracture zones (thin black) (Matthews et al., 2011), aseismic ridges (grey unfilled polygons), coastlines (light-grey), and non-oceanic regions (dark-grey).

Figure 4. (A) Overview of the major spreading systems in the eastern Pacific modified from Wright et al. (2016). (B) Updated spreading systems in the Panama Isthmus region based on this study. Plate boundaries are modified from Bird (2003), fracture zones from Matthews et al. (2011) (thin black), coastlines (light-grey), and non-oceanic regions (dark-grey). Rivera microplate (R); Galapagos microplate (GA); Easter microplate (EA); Juan Fernandez microplate

(JZ); Sandra rift spreading (San.); Buenaventura rift spreading (Bue.); Malpelo rift spreading (Mal.); Mathematician microplate (Math.).

Figure 5. Tectonic reconstruction of Central American arc blocks from 38 Ma to recent. The Campanian to Eocene belt, and the Oligocene and younger arc ages and locations from Montes et al. (2012). Arrow symbols show direction of rotation of individual blocks according to Montes et al. (2012). Reconstructed continental crust (dark-grey), coastlines (light-grey), ridges and transform faults (black), subduction zones (toothed).

Figure 6. Updated kinematic model and corresponding paleo-age-grid from 35 to present-day. Reconstructed continental crust (dark-grey), coastlines (light-grey), subduction zones (black lines with filled teeth), ridges (black lines), flat slab geometries (thin black lines with unfilled teeth), extinct ridges (thin black lines), topology network polygons (white and dark grey lines), isochrons (thin grey lines) and fracture zones (white). Caribbean (Car); East Pacific Rise (EPR); Pacific (Par); Cocos-Nazca Spreading (CNS); South America (SAM); Bauer Microplate (BM); North America (NAM); Malpelo Microplate (MM); Malpelo Rift (MR); Sandra Rift (SR); Mathematician (M).

Figure 7. (Top) Upper mantle subducted slab material and slab windows at 15 Ma, (middle) 8 Ma and (bottom) 0 Ma for three alternative plate reconstructions: (left) our model, (centre) Müller et al. (2016) and (right) Shephard et al. (2013). The age of the slab volumes are plotted according to colour and depth is plotted according to size. Pink lines denote ridge and transforms and black toothed lines are subduction zones. Grey filled areas denote the size and shape of the slab window and black lines denote their boundaries.

Figure 8. (Left) Location map showing profiles 1-4 sampled for the seismic tomography survey and (right) tomographic profiles from Li et al. (2008) global P-wave tomography model. Colour

indicates anomalies in seismic wave speed as a ±0.8% deviation from average mantle velocities, indicative of subducted slab material (blue), or regions of upwelling (red). North America (NAM); South America (SAM); Cocos-Nazca spreading (CNS).

Figure 9. Comparison of kinematic models with age-coded MIT-P08 mantle tomography (Li et al., 2008). Colour indicates anomalies in seismic wave speed as a ±0.8% deviation from average mantle velocities, indicative of subducted slab material (blue), or regions of upwelling (red). Left, our model; centre, Müller et al. (2016); right, Shephard et al. (2013). Coastlines (grey), subduction zones (toothed), ridges and transform faults (red).

Figure 10. (Top) Major records associated with Central American Seaway closure from the Oligocene. (Bottom) Updated kinematic model including slab window formation (pink) and flat slab geometries (thin black lines with unfilled teeth). Reconstructed continental crust (dark-grey), coastlines (light-grey), subduction zones (black lines with filled teeth), ridges and transform faults (black) and aseismic ridges (grey unfilled polygons). Montes et al. 2012 (1); Bacon et al. 2015 (2); Farris et al. 2011 (3); O'Dea et al. 2016 (4); Montes et al. 2015 (5); Coates et al. 2004 (6); Keigwin 1982 (7); Newkirk and Martin 2009 (8); Lear et al. 2003 (9); Rogers et al. 2002 (10); Gazel et al. 2011 (11); Gutscher et al. 2000 (12); Wagner et al. 2017 (13); de Boer et al. 1995 (14); Johnston and Thorkelson 1997 (15); Haug et al. 2001 (16); Kameo and Sato 2000 (17); Bartoli et al. 2005 (18); Miller et al. 2005 (19); Marshall et al. 1982 (20).

[1]GSA Data Repository item 201Xxxx, GitHub repository link to plate motion model (GPlates) and slab-tracker python code, plate reconstruction methodology and supplementary figures are available online at www.geosociety.org/pubs/ft20XX.htm, or on request from editing@geosociety.org or Documents Secretary, GSA, P.O. Box 9140, Boulder, CO 80301, USA.

1210

Figure 1

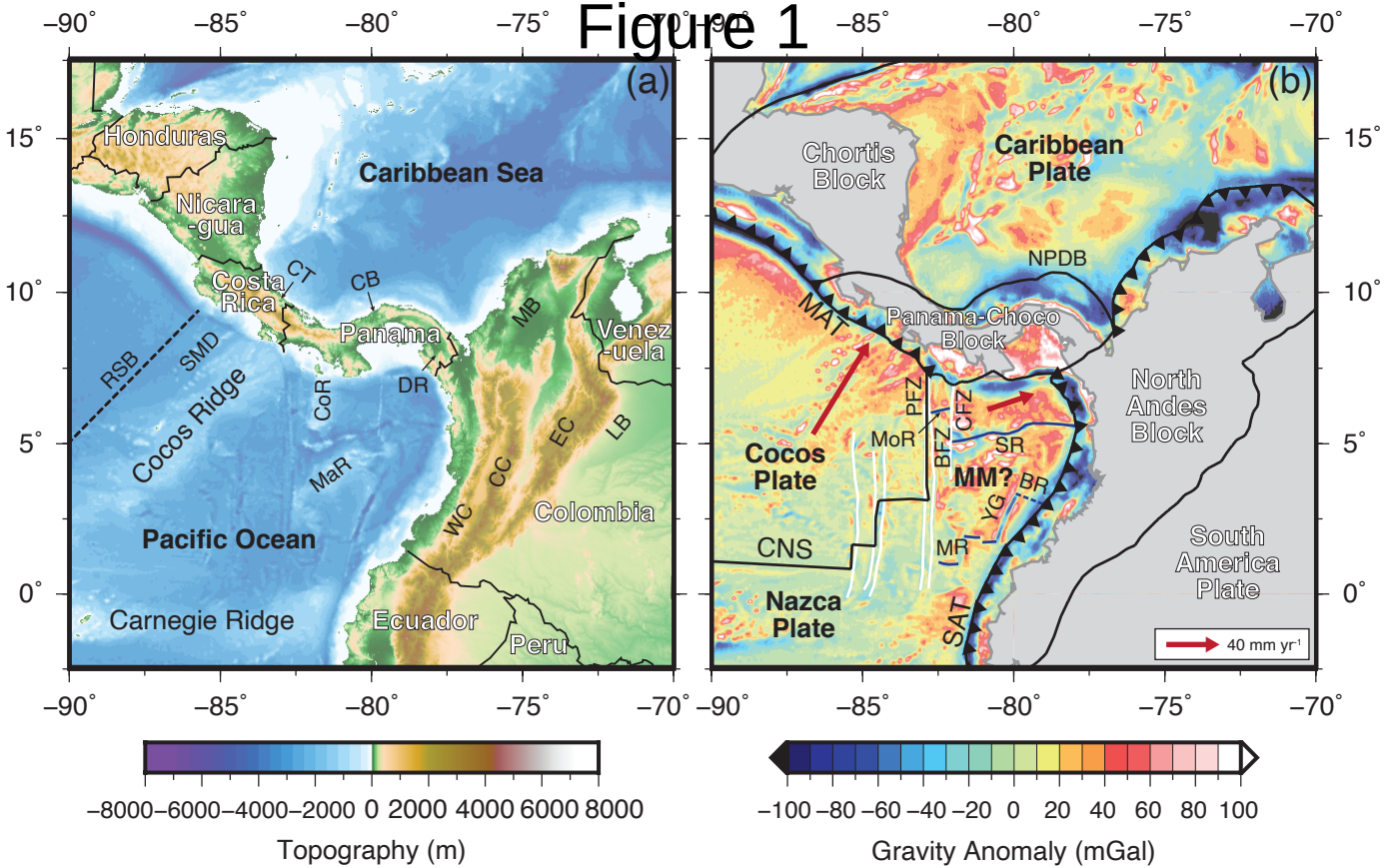
(a)
(b)
Honduras
Nicara
-gua
Costa
Rica
Panama
Caribbean Sea
Venez
-uela
Colombia
Ecuador
Peru
Pacific Ocean
Carnegie Ridge
Cocos Ridge
RSB
SMD
CoR
MaR
CT
CB
DR
MB
EC
CC
WC
LB
Chortis
Block
Caribbean
Plate
NPDB
MAT
Panama-Choco
Block
North
Andes
Block
Cocos
Plate
PFZ
CFZ
BFZ
MoR
SR
MM?
BR
YG
MR
CNS
Nazca
Plate
SAT
South
America
Plate
40 mm yr⁻¹
−90˚
−85˚
−80˚
−75˚
−70˚
15˚
10˚
5˚
0˚
−8000 −6000 −4000 −2000 0 2000 4000 6000 8000
Topography (m)
−100 −80 −60 −40 −20 0 20 40 60 80 100
Gravity Anomaly (mGal)

Figure 2

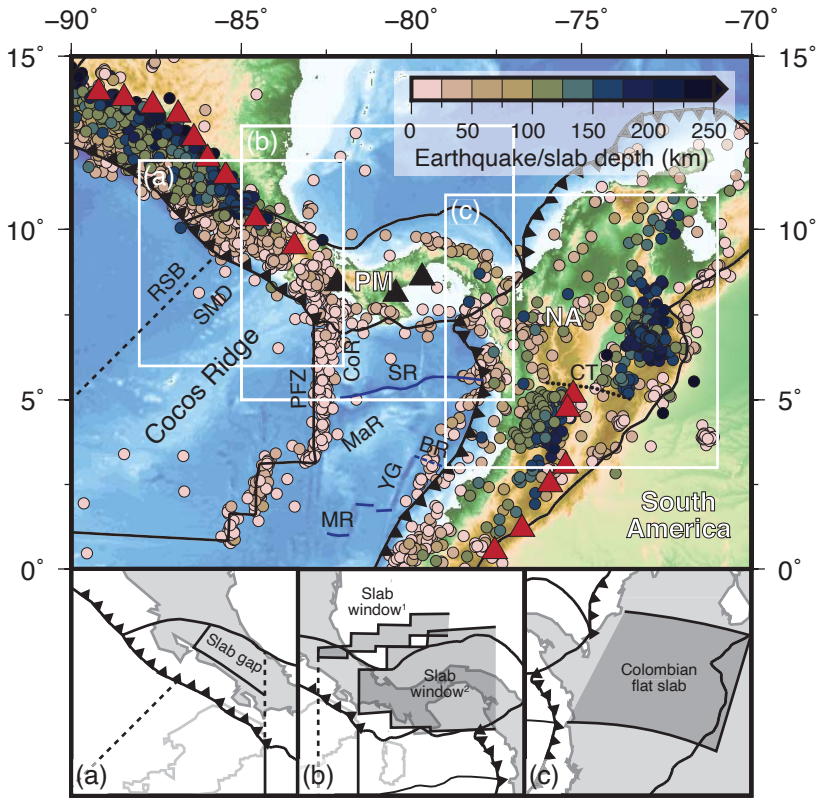
−90°
−85°
−80°
−75°
−70°
15°
10°
5°
0°
0
50
100
150
200
250
Earthquake/slab depth (km)
(a)
(b)
(c)
RSB
SMD
Cocos Ridge
PFZ
CoR
PM
SR
MaR
YG
BB
MR
NA
CT
South America
Slab gap
Slab window¹
Slab window²
Colombian flat slab

Figure 3

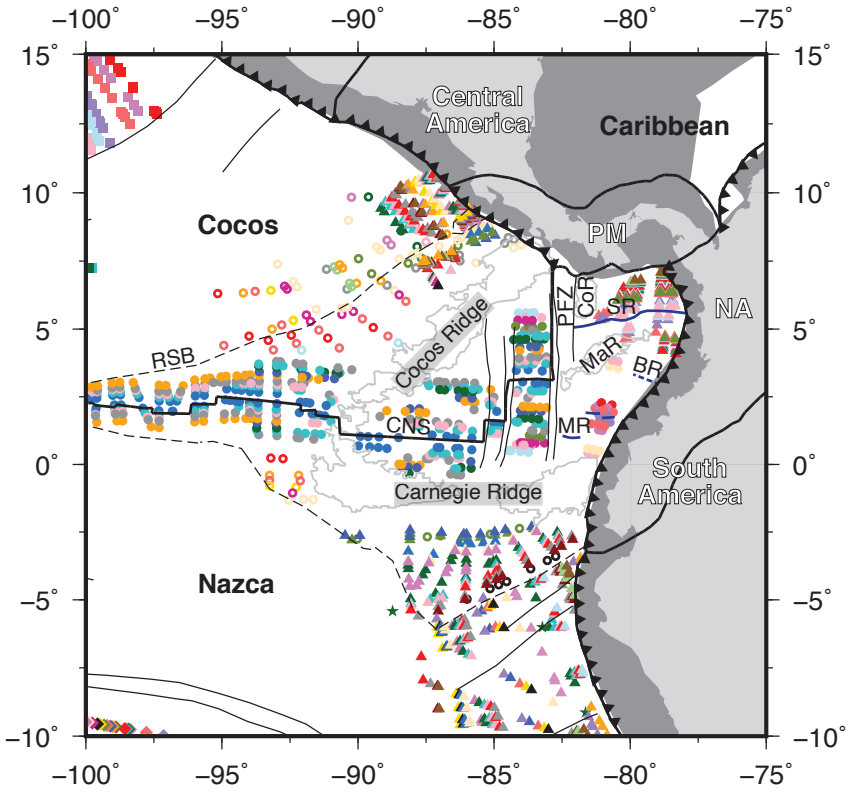

Reference

- Atwater & Severinghaus (1989)
- Barckhausen et al. (2001)
- Eakins & Lonsdale (2003)
- Handschumacher et al. (1976)
- Klitgord & Mammerickx (1982)
- Lonsdale (2005)

Chron

- 1y, 3n2o, 4n2y, 5r2r-1y, 5ADy, 5Dr1o, 6Bn1o, 8n1y
- 1o, 3n2y, 4n2c, 5r2r-1o, 5ADc, 5Ey, 6Bn2y, 8n1o
- 1r1y, 3n3o, 4n2o, 5r2y, 5ADo, 5Ec, 6Bn2c, 8n2y
- 1r1o, 3n4y, 4r1y, 5r2o, 5Bn1y, 5Eo, 6Bn2o, 8n2o
- 1r2y, 3n4m, 4r1o, 5An1y, 5Bn1o, 6y, 6Cn1y, 9y
- 2y, 3n4o, 4r2r-1y, 5An1o, 5Bn2y, 6o, 6Cn1o, 9o
- 2m, 3An1y, 4r2r-1o, 5An2y, 5Bn2c, 6An1y, 6Cn2y, 10n1y
- 2o, 3An1m, 4Ay, 5An2c, 5Bn2o, 6An1o, 6Cn2o,10n1o
- 2r1y, 3An1o, 4Ac, 5An2o, 5Cn1y, 6An2y, 6Cn3y, 10n2y
- 2r1o, 3An2y, 4Ao, 5Ar1y, 5Cn1c, 6An2c, 6Cn3o, 10n2o
- 2An1y, 3An2o, 4Ar1y, 5Ar1o, 5Cn1o, 6An2o, 6Cn3o, 11n1y
- 2An1o, 3By, 4Ar1o, 5Ar2y, 5Cn2y, 6AAy, 7n1y, 11n1o
- 2An2y, 3Bc, 4Ar2y, 5Ar2o, 5Cn2o, 6AAc, 7n1c, 11n2y
- 2An2o, 3Bo, 4Ar2o, 5AAy, 5Cn3y, 6AAo, 7n1o, 11n2o
- 2An3y, 3Br1y, 5n1y, 5AAc, 5Cn3c, 6AAr1y, 7n2y, 12y
- 2An3o, 3Br1o, 5n1o, 5AAo, 5Cn3o, 6AAr1o, 7n2c, 12o
- 3n1y, 3Br2y, 5n2y, 5ABy, 5Dy, 6AAr2y, 7n2o
- 3n1m, 5Br2o, 5n2o, 5ABo, 5Dc, 6AAr2c, 7Ay
- 3n1o, 4n1o, 5r1y, 5ACy, 5Do, 6AAr2o, 7Ac
- 3n2y, 4n1o, 5ACo, 5Dr1y, 6Bn1y, 7Ao

Figure 4

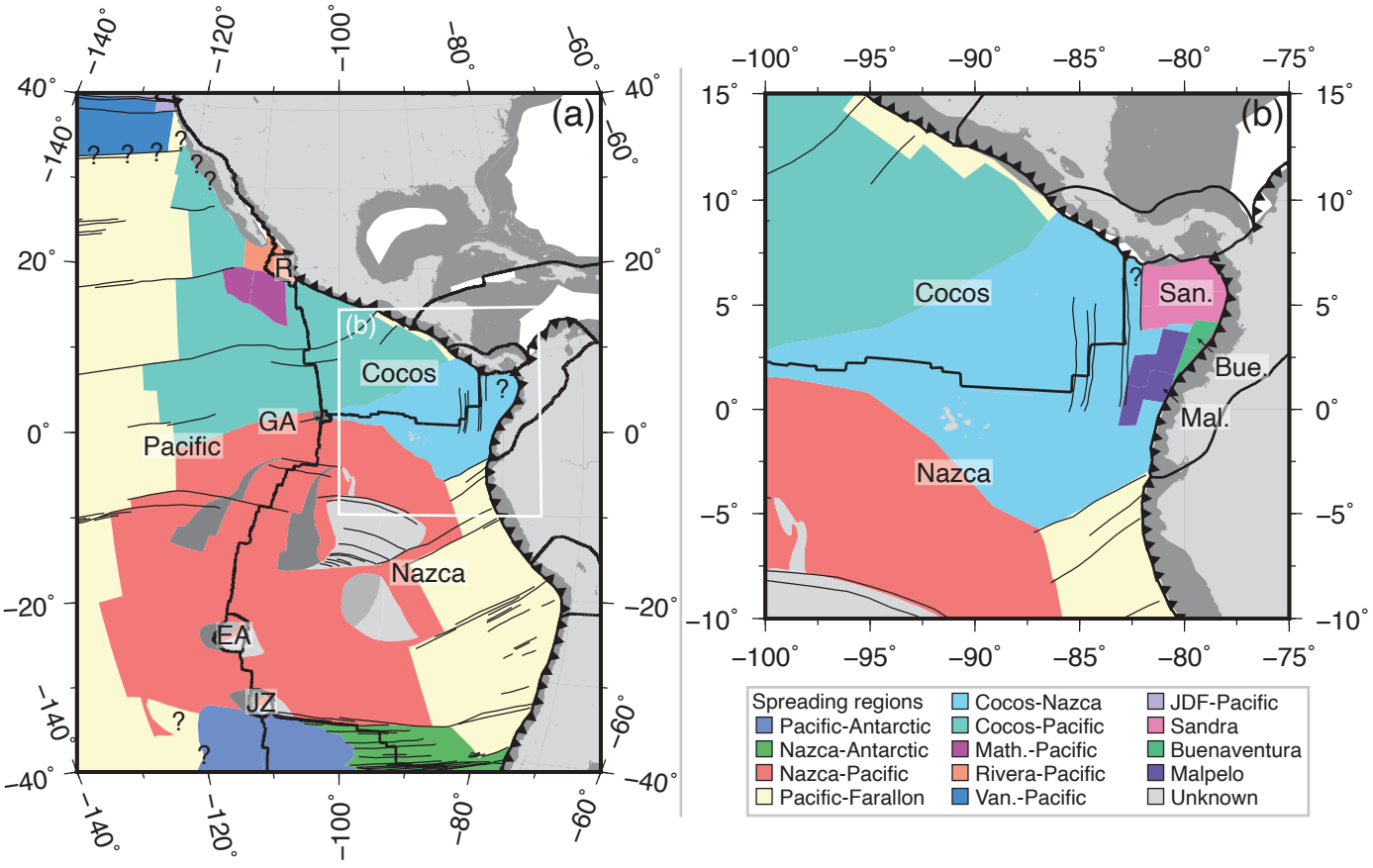
(a)
(b)
Cocos
Pacific
Nazca
GA
EA
JZ
R
?
−140°
−120°
−100°
−80°
−60°
40°
20°
0°
−20°
−40°
(b)
Cocos
Nazca
San.
Bue.
Mal.
−100°
−95°
−90°
−85°
−80°
−75°
15°
10°
5°
0°
−5°
−10°
Spreading regions
Pacific-Antarctic
Nazca-Antarctic
Nazca-Pacific
Pacific-Farallon
Cocos-Nazca
Cocos-Pacific
Math.-Pacific
Rivera-Pacific
Van.-Pacific
JDF-Pacific
Sandra
Buenaventura
Malpelo
Unknown

Figure 5

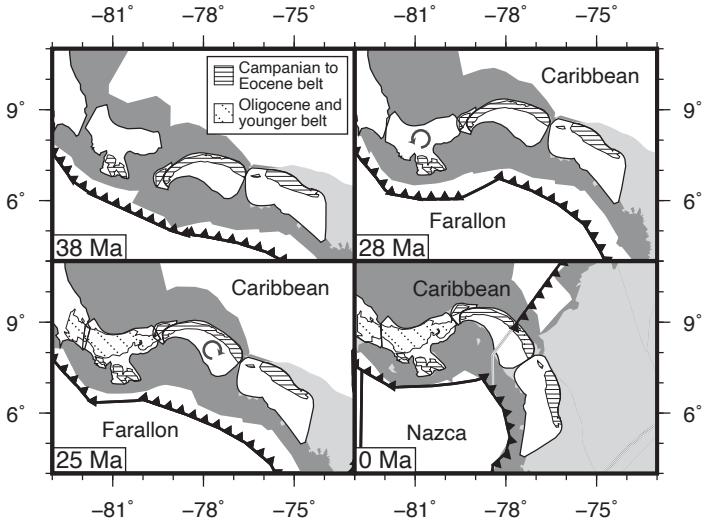
−81°
−78°
−75°
9°
6°
Campanian to Eocene belt
Oligocene and younger belt
38 Ma
Caribbean
Farallon
28 Ma
Caribbean
Farallon
25 Ma
Caribbean
Nazca
0 Ma

Figure 6a

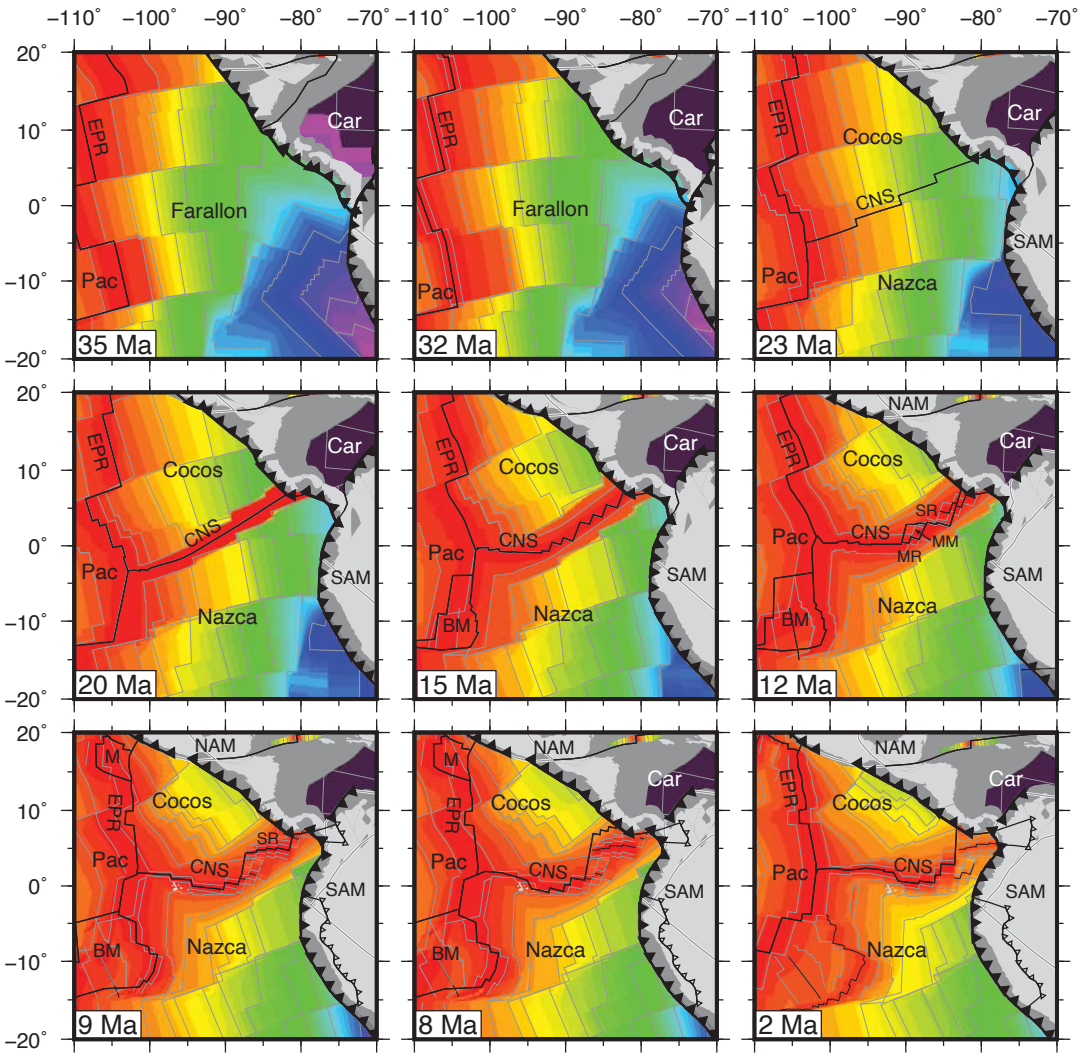
−110° −100° −90° −80° −70°
20° 10° 0° −10° −20°
35 Ma
Car
EPR
Farallon
Pac
32 Ma
Car
EPR
Farallon
Pac
23 Ma
Car
EPR
Cocos
CNS
SAM
Pac
Nazca
20 Ma
Car
EPR
Cocos
CNS
Pac
SAM
Nazca
15 Ma
Car
EPR
Cocos
CNS
Pac
SAM
BM
Nazca
12 Ma
NAM
Car
EPR
Cocos
SR
Pac
CNS
MM
MR
SAM
BM
Nazca
9 Ma
NAM
M
EPR
Cocos
SR
Pac
CNS
SAM
BM
Nazca
8 Ma
NAM
Car
M
EPR
Cocos
Pac
CNS
SAM
BM
Nazca
2 Ma
NAM
Car
EPR
Cocos
Pac
CNS
SAM
Nazca

Figure 6b

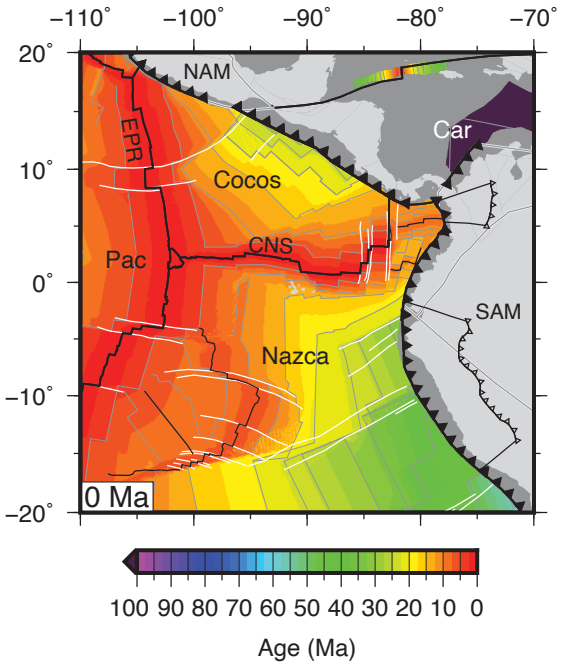
−110°
−100°
−90°
−80°
−70°
20°
10°
0°
−10°
−20°
NAM
Car
EPR
Cocos
CNS
Pac
SAM
Nazca
0 Ma
100 90 80 70 60 50 40 30 20 10 0
Age (Ma)

Figure 7

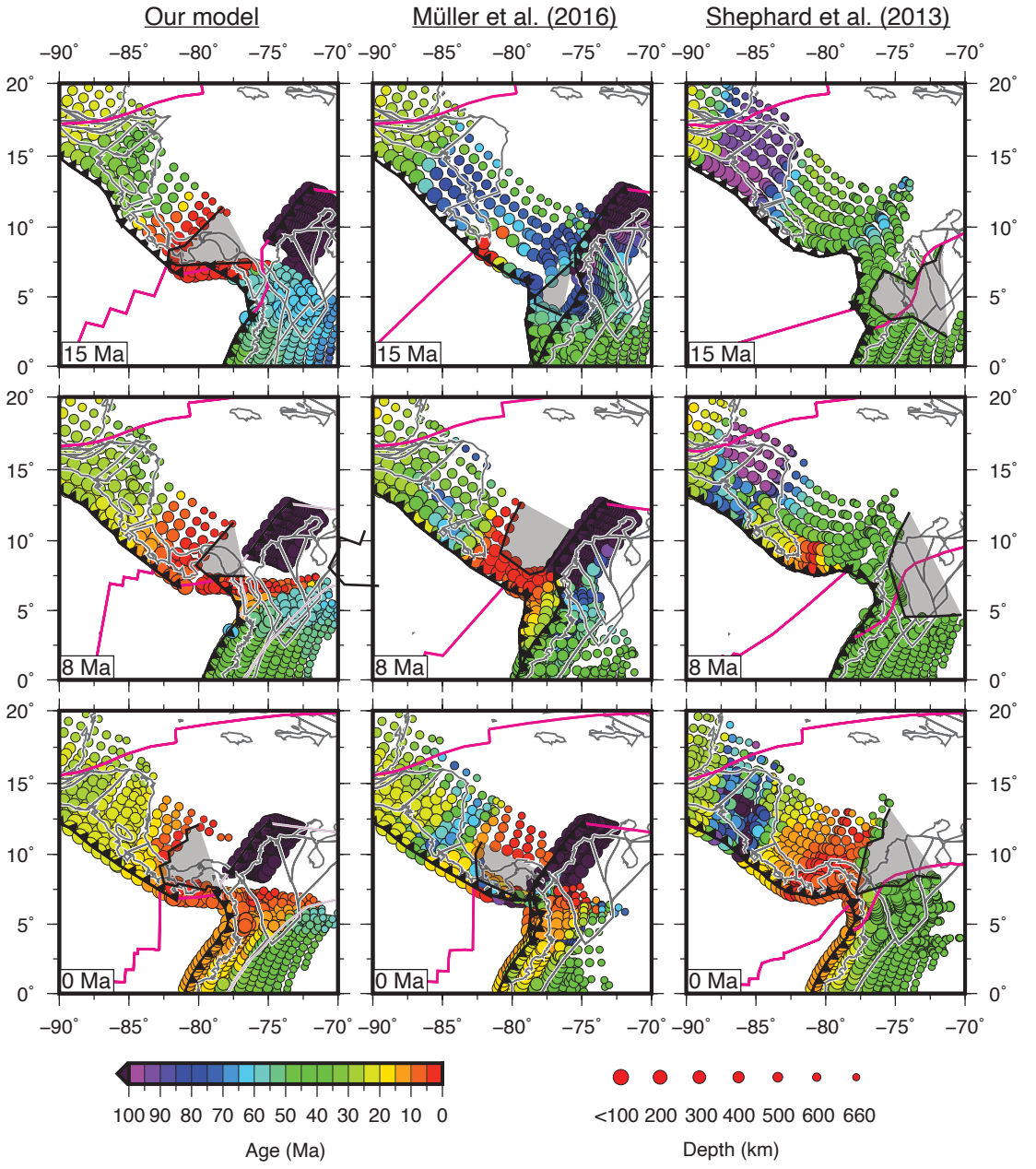
Our model
Müller et al. (2016)
Shephard et al. (2013)
−90° −85° −80° −75° −70°
20° 15° 10° 5° 0°
15 Ma
8 Ma
0 Ma
100 90 80 70 60 50 40 30 20 10 0
Age (Ma)
<100 200 300 400 500 600 660
Depth (km)

Figure 8

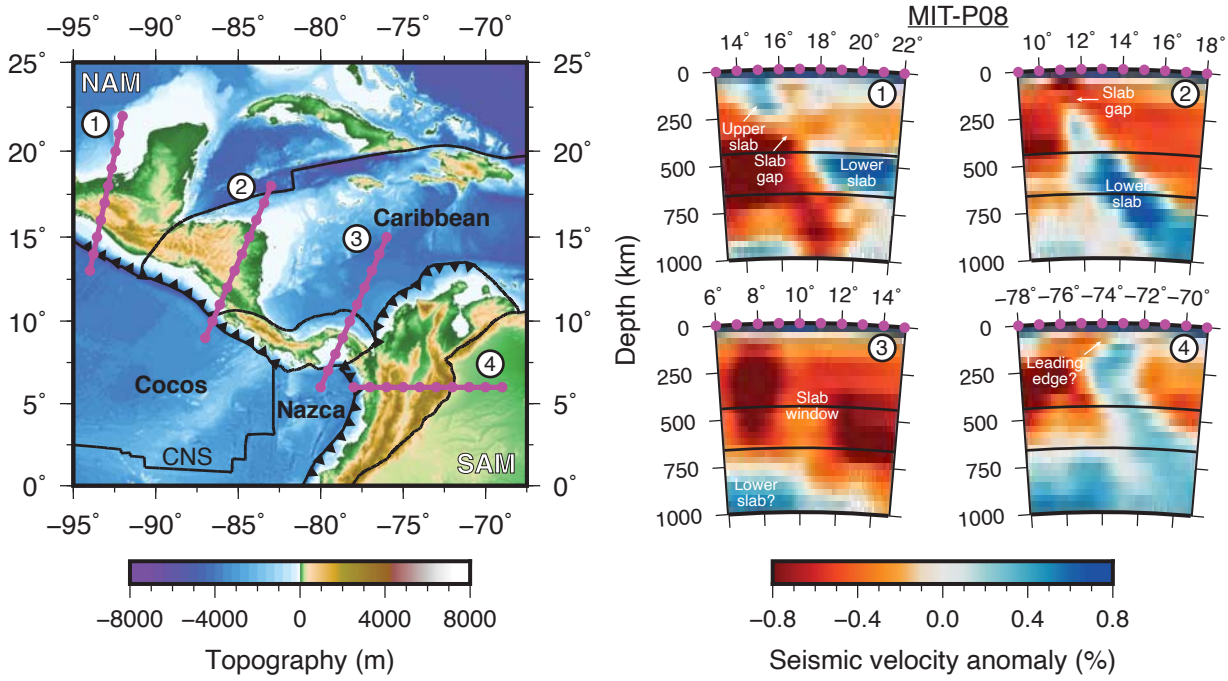
NAM
Caribbean
Cocos
Nazca
CNS
SAM
Topography (m)
MIT-P08
Depth (km)
Upper slab
Slab gap
Lower slab
Slab window
Lower slab?
Leading edge?
Seismic velocity anomaly (%)

Figure 9

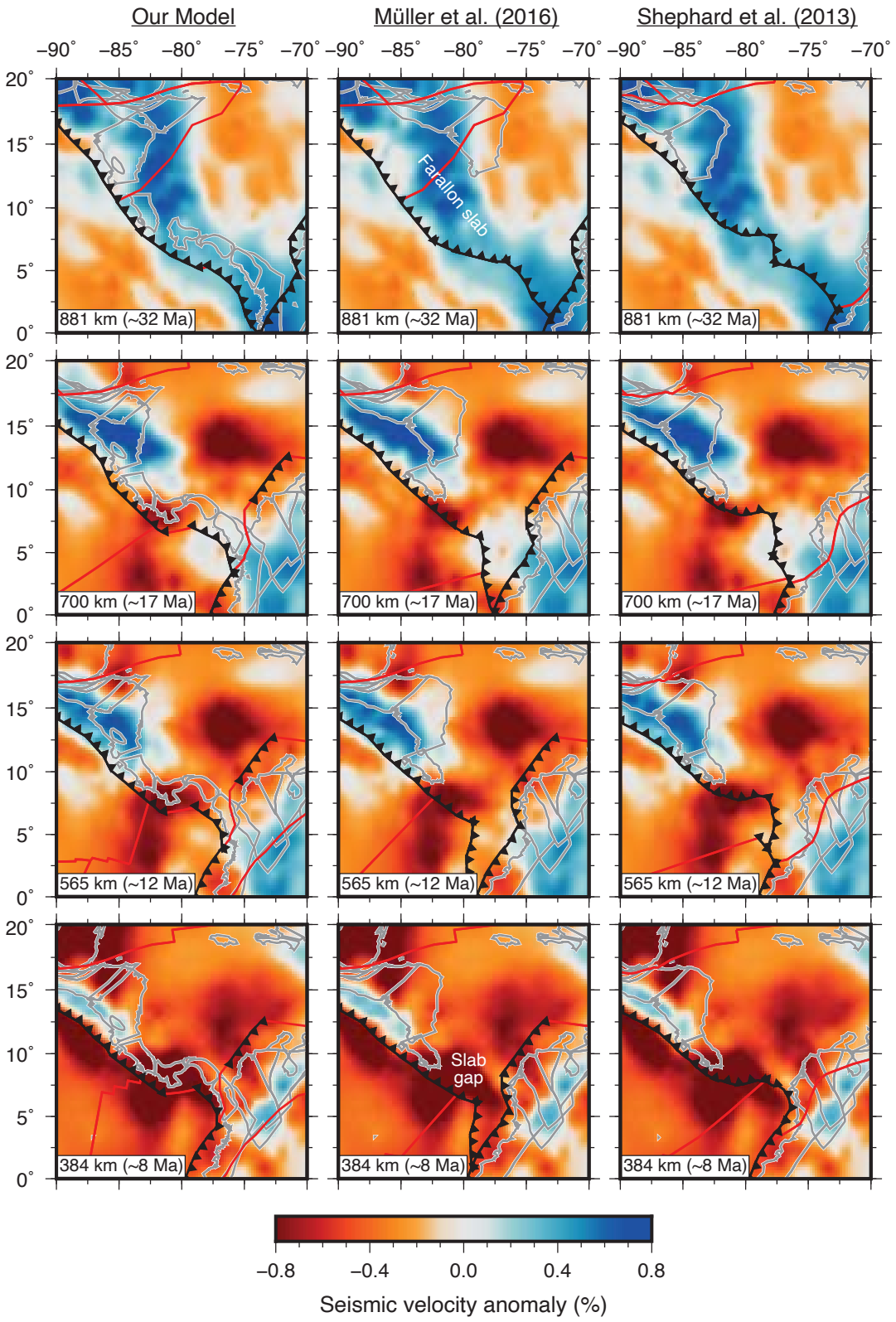
Our Model
Müller et al. (2016)
Shephard et al. (2013)
−90° −85° −80° −75° −70°
20° 15° 10° 5° 0°
Farallon slab
Slab gap
881 km (~32 Ma)
700 km (~17 Ma)
565 km (~12 Ma)
384 km (~8 Ma)
−0.8 −0.4 0.0 0.4 0.8
Seismic velocity anomaly (%)

Figure 10

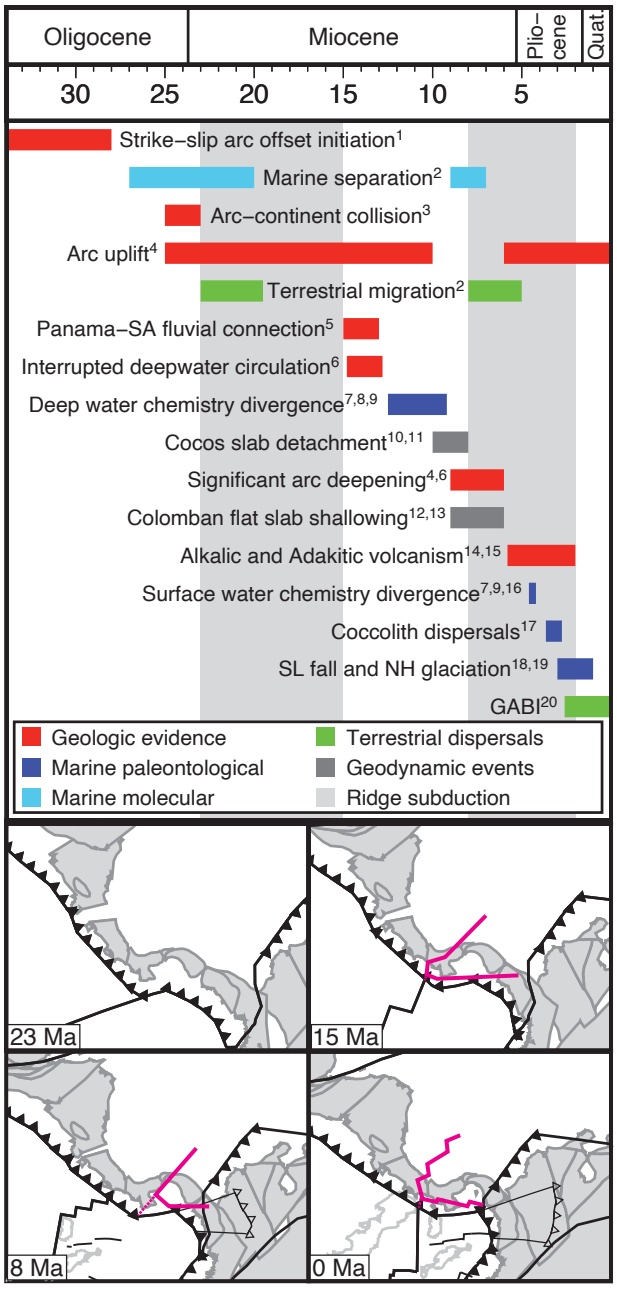
Oligocene
Miocene
Plio–cene
Quat
30
25
20
15
10
5
Strike–slip arc offset initiation[1]
Marine separation[2]
Arc–continent collision[3]
Arc uplift[4]
Terrestrial migration[2]
Panama–SA fluvial connection[5]
Interrupted deepwater circulation[6]
Deep water chemistry divergence[7,8,9]
Cocos slab detachment[10,11]
Significant arc deepening[4,6]
Colomban flat slab shallowing[12,13]
Alkalic and Adakitic volcanism[14,15]
Surface water chemistry divergence[7,9,16]
Coccolith dispersals[17]
SL fall and NH glaciation[18,19]
GABI[20]
Geologic evidence
Marine paleontological
Marine molecular
Terrestrial dispersals
Geodynamic events
Ridge subduction
23 Ma
15 Ma
8 Ma
0 Ma